48. Gardiner, K. J. Molecular basis of pharmacotherapies for cognition in Down syndrome. *Trends Pharmacol. Sci.* **31,** 66–73 (2009).
49. Yu, T. *et al.* A mouse model of Down syndrome trisomic for all human chromosome 21 syntenic regions. *Hum. Mol. Genet* **19,** 2780–2791.
50. Kimura, R. *et al.* The DYRK1A gene, encoded in chromosome 21 Down syndrome critical region, bridges between β-amyloid production and tau phosphorylation in Alzheimer disease. *Hum. Mol. Genet.* **16,** 15–23 (2007).
51. Ferrer, I. *et al.* Constitutive Dyrk1A is abnormally expressed in Alzheimer disease, Down syndrome, Pick disease, and related transgenic models. *Neurobiol. Dis.* **20,** 392–400 (2005).
52. Wisniewski, K. E., Wisniewski, H. M. & Wen, G. Y. Occurrence of neuropathological changes and dementia of Alzheimer's disease in Down's syndrome. *Ann. Neurol.* **17,** 278–282 (1985).
53. Leder, S., Weber, Y., Altafaj, X., Estivill, X., Joost, H. G. & Becker, W. Cloning and characterization of DYRK1B, a novel member of the DYRK family of protein kinases. *Biochem. Biophys. Res. Commun.* **254,** 474–479 (1999).
54. Fukuhara, T. *et al.* Utilization of host SR protein kinases and RNA-splicing machinery during viral replication. *Proc. Natl Acad. Sci. USA* **103,** 11329–11333 (2006).
55. McCoy, A. J., Grosse-Kunstleve, R. W., Adams, P. D., Winn, M. D., Storoni, L. C. & Read, R. J. Phaser crystallographic software. *J. Appl. Crystallogr.* **40,** 658–674 (2007).
56. Brunger, A. T. Version 1.2 of the crystallography and NMR system. *Nat. Protoc.* **2,** 2728–2733 (2007).
57. Hyodo-Miura, J., Urushiyama, S., Nagai, S., Nishita, M., Ueno, N. & Shibuya, H. Involvement of NLK and Sox11 in neural induction in Xenopus development. *Genes Cells* **7,** 487–496 (2002).
58. Satoh, K. *et al.* Nemo-like kinase-myocyte enhancer factor 2A signaling regulates anterior formation in Xenopus development. *Mol. Cell Biol.* **27,** 7623–7630 (2007).

Acknowledgments

We thank Professor Dr Hidenori Ichijo for the ASK1 expression vector, M Ishikawa for the HRMS analysis and Dr Yukiko Okuno for technical and bibliographical assistance. We also thank the laboratory members for their critical comments and discussion. This work was supported by Grants-in-aid (MH) from Japan Science and Technology Agency and the Ministry of Education, Culture, Sports, Science, and Technology of Japan.

Author contributions

Y.O., T.H. and M.H. designed the study. All authors contributed to the preparation of the paper, which was finalized by Y.O., T.H. and M.H. T.H. and T.H. synthesized the molecules. M.Y., Y.N. and H.O. determined the IC_{50} values and performed the MAOA assay, HPLC analysis and single-concentration kinase inhibition assays using radioisotope. Y.O. determined the K_m and K_i values and performed the in-cell kinase assay, NFAT localization assay and dual luciferase reporter assay. Y.N., T.I. and N.I. determined the structures of Dyrk1A/inhibitor co-crystals and analysed the hypothetical MAOA/inhibitor complex. E.O., T.G., I.K. and H.S. performed the *Xenopus* experiments.

Additional information

Supplementary Information accompanies this paper on http://www.nature.com/naturecommunications

Competing financial interests: The authors declare no competing financial interests.

Reprints and permission information is available online at http://npg.nature.com/reprintsandpermissions/

How to cite this article: Ogawa, Y. *et al.* Development of a novel selective inhibitor of the Down syndrome-related kinase Dyrk1A. *Nat. Commun.* 1:86 doi: 10.1038/ncomms1090 (2010).

ANTIMICROBIAL AGENTS AND CHEMOTHERAPY, Aug. 2010, p. 3179–3186 Vol. 54, No. 8
0066-4804/10/$12.00 doi:10.1128/AAC.00113-10

Inhibition of Hepatitis C Virus Replication by a Specific Inhibitor of Serine-Arginine-Rich Protein Kinase▽

Yuko Karakama,[1]§ Naoya Sakamoto,[1,2]§* Yasuhiro Itsui,[1,5] Mina Nakagawa,[1,2] Megumi Tasaka-Fujita,[1] Yuki Nishimura-Sakurai,[1] Sei Kakinuma,[1,2] Masaya Oooka,[3] Seishin Azuma,[1] Kiichiro Tsuchiya,[1] Hiroshi Onogi,[4] Masatoshi Hagiwara,[4] and Mamoru Watanabe[1]

Department of Gastroenterology and Hepatology[1] and Department for Hepatitis Control,[2] Tokyo Medical and Dental University, Tokyo, Japan; Department of General Medicine, Tokyo Medical and Dental University, Tokyo, Japan[3]; Department of Functional Genomics, Medical Research Institute, Tokyo Medical and Dental University, Tokyo, Japan[4]; and Department of Internal Medicine, Soka Municipal Hospital, Saitama, Japan[5]

Received 26 January 2010/Returned for modification 9 March 2010/Accepted 11 May 2010

Splicing of messenger RNAs is regulated by site-specific binding of members of the serine-arginine-rich (SR) protein family, and SR protein kinases (SRPK) 1 and 2 regulate overall activity of the SR proteins by phosphorylation of their RS domains. We have reported that specifically designed SRPK inhibitors suppressed effectively several DNA and RNA viruses *in vitro* and *in vivo*. Here, we show that an SRPK inhibitor, SRPIN340, suppressed in a dose-dependent fashion expression of a hepatitis C virus (HCV) subgenomic replicon and replication of the HCV-JFH1 clone *in vitro*. The inhibitory effects were not associated with antiproliferative or nonspecific cytotoxic effects on the host cells. Overexpression of SRPK1 or SRPK2 resulted in augmentation of HCV replication, while small interfering RNA (siRNA) knockdown of the SRPKs suppressed HCV replication significantly. Immunocytochemistry showed that SRPKs and the HCV core and NS5A proteins colocalized to some extent in the perinuclear area. Our results demonstrate that SRPKs are host factors essential for HCV replication and that functional inhibitors of these kinases may constitute a new class of antiviral agents against HCV infection.

Hepatitis C virus (HCV) infects up to 170 million people worldwide, and these infections frequently are characterized by chronic liver inflammation, leading to decompensated liver cirrhosis and hepatocellular cancers (1). Alpha and beta interferons are the mainstay of HCV therapeutics. However, the most effective pegylated interferon plus ribavirin combination therapies can eliminate HCV from around half of the patients only (6). These difficulties in eradicating HCV are compounded by the limited treatment options. For this reason, the development of safe and effective therapeutic agents against HCV has been a strong motivation in academia and industry (23).

Serine-arginine-rich (SR) proteins are a family of non-small nuclear ribonucleoprotein particle (non-snRNP) splicing factors that are highly conserved throughout the eukaryotes. They harbor one or two RNA recognition motifs and an RS domain at the amino and carboxyl termini, respectively (29). RS domains consist of multiple consecutive Arg-Ser/Ser-Arg dipeptide repeats, in which the Ser residues are extensively phosphorylated by several kinases, including SR protein kinases (SRPKs). SRPK1 was the first SR protein kinase to be cloned, on the basis of its ability to phosphorylate SR proteins *in vitro* (8, 9), and two other structurally related kinases, SRPK2 and SRPK3, also have been shown to phosphorylate SR proteins (16, 31). Although the precise physiological role of this phosphorylation remains unknown, it is expected that phosphorylation of SR proteins affects their protein-protein and protein-RNA interactions, intracellular localization and trafficking, and alternative splicing of pre-mRNA (21).

As SRPK-dependent herpes simplex virus (HSV) splicing and SRPK-mediated phosphorylation of hepatitis B virus (HBV) core protein have been reported (4, 25, 33), it is reasonable to expect that SR proteins and SRPK might be suitable targets for therapeutic modulation of various viral infections. Actually, we found that increased activity of SRPK2 upregulated human immunodeficiency virus (HIV) expression and that an isonicotinamide compound, SRPIN340, which preferentially inhibited SRPK1 and SRPK2, suppressed propagation of Sindbis virus, HIV, and cytomegalovirus (7). In this study, we investigated the effects of SRPIN340 on HCV replication using the HCV subgenomic replicon system (27, 32) and HCV-JFH1 virus cell culture (30, 34). Here, we demonstrate that cellular SRPK is required for HCV replication and suggest that the inhibitor of SRPK could be used therapeutically.

MATERIALS AND METHODS

SRPK inhibitor. SRPIN340, *N*-[2-(1-piperidinyl)-5-(trifluoromethyl)phenyl] isonicotinamide, inhibits SRPK1 and SRPK2 kinase activities potently (7). SRPIN340 does not inhibit other classes of SRPKs significantly, including Clk1 and Clk and other classes of SR kinases. SRPIN614, *N*-methyl-*N*-[2-(1-piperidinyl)-5-(trifluoromethyl)phenyl]isonicotinamide, is a negative-control compound that has no suppressive effects on SRPK1 or SRPK2. SRPIN340 and SRPIN614 were synthesized in-house (7).

***In vitro* kinase assay.** Kinase activities of SRPKs were assayed as described previously (18). Briefly, His_6-tagged recombinant SRPK1 or SRPK2 was expressed in *Escherichia coli* and purified by Ni-nitrilotriacetic acid (NTA) affinity chromatography. The purified SRPK1 or SRPK2 was incubated in the presence of ATP, [γ-^{32}P]ATP, and a synthetic peptide of the SF2/ASF RS domain (NH_2-RSPSYGRSRSRSRSRSRSRSNSRSRSY-OH) at pH 7.5 and 30°C for 10 min. The reaction mixtures were spotted onto phosphocellulose membranes (What-

* Corresponding author. Mailing address: Department of Gastroenterology and Hepatology, Tokyo Medical and Dental University, 1-5-45 Yushima, Bunkyo-ku, Tokyo 113-8519, Japan. Phone: 81 3-5803-5877. Fax: 81 3-5803-0268. E-mail: nsakamoto.gast@tmd.ac.jp.
§ Y.K. and N.S. contributed equally to this work.
▽ Published ahead of print on 24 May 2010.

man, Kent, United Kingdom) and washed with 5% phosphoric acid solution, and the radioactivity was measured using a liquid scintillation counter. The net radioactivity was deduced by subtracting the background count from the reaction mixture without kinase, and the data are expressed as the percentage of the control sample containing the solvent.

Cells and cell culture. Huh7 and Huh7.5.1 cell lines (34) were maintained in Dulbecco's modified minimal essential medium (Sigma, St. Louis, MO) supplemented with 10% fetal calf serum at 37°C under 5% CO_2. To maintain cell lines carrying the HCV replicon (Huh7/Rep-Feo cells), G418 (Nacalai Tesque, Kyoto, Japan) was added to the culture medium to a final concentration of 500 μg/ml.

HCV replicon constructs and transfection. The HCV replicon plasmids, which contain Rep-Feo, were derived from the HCV-N strain (pHC1bneo/delS [Rep-Feo-1b]) and the HCV-JFH1 strain (pSGR-JFH1 [Rep-Feo-2a]) (10, 14). These constructs express a chimeric reporter protein of firefly luciferase (Fluc) and neomycin phosphotransferase. RNA synthesis and transfection of the replicon have been described (Huh7/Rep-Feo-1b, Huh7/Rep-Feo-2a) (27, 32).

HCV cell culture system. A plasmid, pJFH1-full (30, 34), which encodes the full-length HCV-JFH1 sequence, was linearized and used as the template for synthesis of HCV RNA using the RiboMax large-scale RNA production system (Promega, Madison, WI) (26). After DNase I (RQ-1, RNase-free DNase, Promega) treatment, the transcribed HCV RNA was purified using ISOGEN (Nippon Gene, Tokyo, Japan). For the RNA transfection, Huh7.5.1 cells were washed twice, and 5×10^6 cells were suspended in Opti-MEM I (Invitrogen, Carlsbad, CA) containing 10 μg of HCV RNA, transferred into a 4-mm electroporation cuvette, and subjected to an electric pulse (1,050 μF and 270 V) using the Easy Ject system (EquiBio, Middlesex, United Kingdom). After electroporation, the cell suspension was left for 5 min at room temperature and then incubated under normal culture conditions in a 10-cm-diameter cell culture dish. The transfected cells were split every 3 to 5 days. The culture supernatants were subsequently transferred onto uninfected Huh7 cells.

RT-PCR. SRPK mRNA was detected by reverse transcription-PCR (RT-PCR) as described previously (12). The primers used were SRPK1-S (5′-GCG AAT GCA GGA AAT TGA GG-3′) and SRPK1-AS (5′-CAT AAG CGT TTG ATC CTG GC-3′) and SRPK2-S (5′-CCC TGC GGA CTA CTG CAA AGG-3′) and SRPK2-AS (5′-CAT TGC AAC AAA TCT TTT CCC-3′).

Luciferase assays. Luciferase activity was measured with a Lumat LM9501 luminometer (Promega) using a Bright-Glo luciferase assay system (Promega) or a Dual-Luciferase reporter assay system (Promega), as described previously (22).

MTS assays. To evaluate cell viability, dimethylthiazol carboxymethoxy-phenyl sulfophenyl tetrazolium (MTS) assays were performed using a CellTiter 96 aqueous one-solution cell proliferation assay kit (Promega), as described previously (24).

Quantification of HCV core antigen in culture media. Culture media from JFH1-RNA-transfected Huh7 cells were collected, passed through a 0.45-μm filter (MILLEX-HA; Millipore, Bedford, MA), and stored at −80°C. The concentrations of core antigen in the culture supernatants were measured using a chemiluminescence enzyme immunoassay (CLEIA) according to the manufacturer's protocol (Lumipulse Ortho HCV antigen; Ortho-Clinical Diagnostics, Tokyo, Japan).

Real-time RT-PCR analysis. The real-time RT-PCR was done as previously described (11). Briefly, total cellular RNA was isolated using ISOGEN (Nippon Gene), reverse transcribed, and subjected to real-time PCR analyses. Expression of mRNA was quantified using the TaqMan universal PCR master mix and the ABI 7500 real-time PCR system (Applied Biosystems, Foster City, CA).

Western blot analysis. Western blotting was performed as described previously (11). Briefly, 10 μg of total cell lysate was separated by SDS-PAGE and blotted onto a polyvinylidene fluoride (PVDF) membrane. The membrane was incubated with the primary antibodies, followed by a peroxidase-labeled anti-IgG antibody, and visualized by chemiluminescence using the ECL Western blotting analysis system (Amersham Biosciences, Buckinghamshire, United Kingdom). The antibodies used were mouse monoclonal anti-HCV-core antibody (Abcam, Cambridge, MA), mouse monoclonal anti-HCV-NS5A antibody (Biodesign), and mouse anti-beta-actin antibody (Sigma).

Indirect immunofluorescence assay. Cells seeded onto tissue culture chamber slides were fixed with cold acetone. The cells were incubated with anti-hemagglutinin (HA) and anti-core or anti-NS5A antibodies and subsequently with Alexa 488- or Alexa 568-labeled secondary antibodies. Cells were mounted with VECTA SHIELD mounting medium and DAPI (4′,6-diamidino-2-phenylindole) (Vector Laboratories) and visualized by fluorescence microscopy (BZ-8000; Keyence) and confocal laser microscopy (FLUOVIEW FV10i; Olympus, Tokyo, Japan).

Synthetic siRNA. The small interfering RNAs (siRNAs) were designed to target SRPK1 and SRPK2. Sequences of SRPK1-directed siRNAs were as follows: no. 1, 5′-UUA AUG ACU UCA AUC ACU CCA UUG C-3′; no. 2, 5′-UAA GAA AUC UGU GAA GCC AGC UGC C-3′. Sequences of SRPK2-directed siRNAs were as follows: no. 3, 5′-AAU ACU GCC UAG CAG CUC UAU GAU G-3′; no. 4, 5′-UCA GCU UGG UGA UGU GUC GCA GUU C-3′. The control siRNA has been described previously (32).

Plasmid constructs. Plasmid pEMCV/IRES/Rluc, which is a renilla luciferase expression plasmid that is driven by an encephalomyocarditis virus internal ribosome entry site (EMCV-IRES), has been described (19). Eukaryote expression plasmids for SRPK1 and SRPK2, pME-HA-SRPK1 and pME-HA-SRPK2, have been described (16).

Calculation of EC_{50}. The 50% effective concentration (EC_{50}) was calculated as the concentration of an inhibitor required for 50% reduction in replicon-based luciferase activity. We used probit regression analysis to obtain values.

Statistical analyses. Statistical analyses were performed using Student's *t* test; *P* values of less than 0.05 were considered statistically significant.

RESULTS

Immunofluorescence microscopy of SRPK and HCV proteins. We first studied the subcellular localization of SRPK1 and SRPK2 and their association with HCV proteins. Expression plasmids for SRPK1 or SRPK2 were transfected into HCV replicon-expressing or HCV-JFH1-infected cells. Immunofluorescence analysis was performed 48 h after transfection (Fig. 1). SRPK1 and SRPK2 were distributed diffusely in the cytoplasm, and HCV core and NS5A proteins were localized at the perinuclear rim and also in the cytoplasm. Although most portions of SRPKs and the viral NS5A and core proteins were localized in different cellular compartments, SRPKs and the HCV core and NS5A proteins colocalized to some extent in the perinuclear area.

SRPIN340 inhibits kinase activities of SRPK1 and SRPK2. The *in vitro* kinase assays showed that SRPIN340 (Fig. 2A) inhibited the kinase activities of SRPK1 and SRPK2. Ten μM SRPIN340 inhibited SRPK1- and SRPK2-mediated phosphorylation of synthetic RS-repeat peptide substrate by 99.2% and 85%, respectively (Fig. 2B), which was consistent with the results of our previous study (7). The K_i value for inhibition of SRPK1 kinase activity was 0.89 μM. SRPIN614, which lacked SRPK inhibitory action, did not inhibit SRPK1 or SRPK2 activity significantly.

SRPK inhibitor effectively suppresses HCV subgenomic replication. Next, we detected expression of SRPK1 and SRPK2 mRNAs in Huh7 cell lines using RT-PCR. As shown in Fig. 2C, both SRPK1 and SRPK2 mRNAs were detectable in Huh7 cells. Next, we assessed the effects of SRPIN340 on replication of the HCV genotype 1b and 2a replicons. SRPIN340 was added to HCV replicon-expressing cells, Huh7/Rep-Feo-1b and Huh7/Rep-Feo-2a. After 48 h of incubation, expression levels of the HCV replicons were measured by luciferase assay. SRPIN340 suppressed HCV 1b and 2a replication in a dose-dependent manner (Fig. 3A). The 50% effective concentrations (EC_{50}) for the HCV 1b and 2a replicons were 4.7 μM and 15.8 μM, respectively. In contrast, SRPIN614, which did not possess SRPK inhibitory activity, did not suppress expression of the replicon even at a concentration of 100 μM. MTS-mediated cell viability assays showed no significant effects of SRPIN340 or SRPIN614 (Fig. 3B). Similarly, we assessed the effect by Western blotting. SRPIN340 suppressed cellular HCV NS5A protein expression levels in a dose-dependent manner (Fig. 3C). SRPIN340 showed no effect on EMCV-IRES-mediated protein expression (Fig. 3D). These results

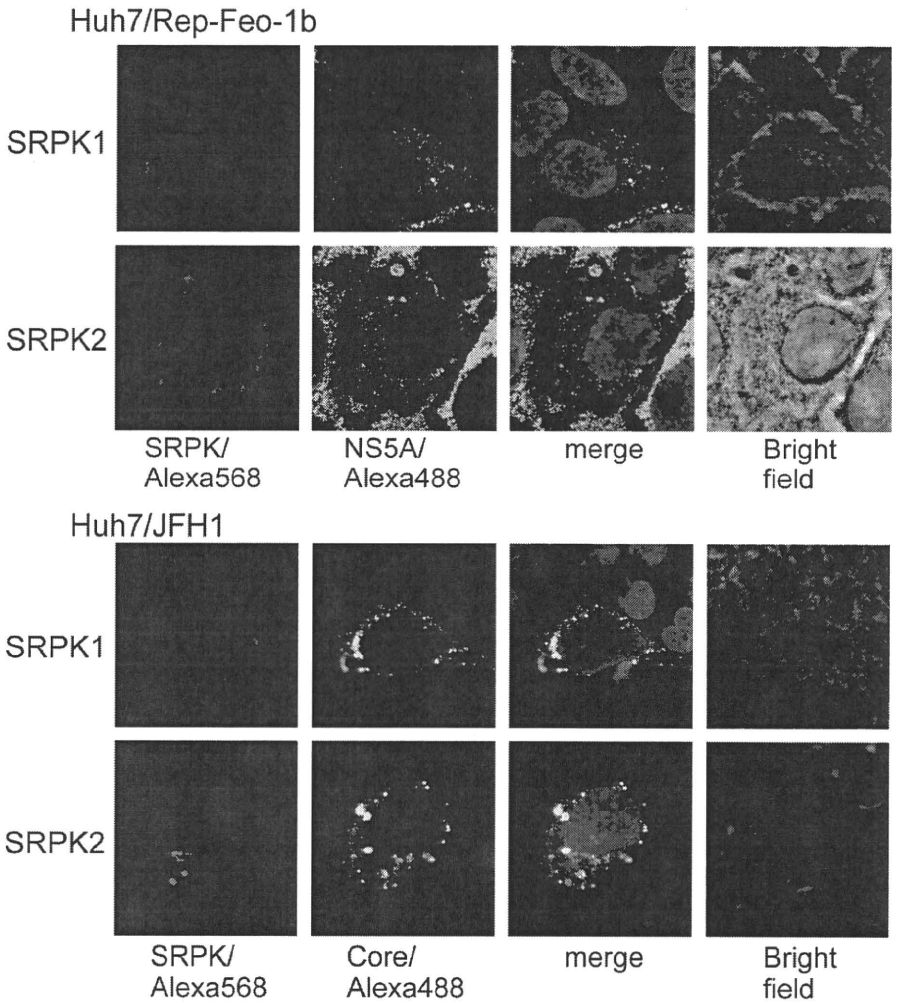

FIG. 1. Immunofluorescence microscopy. Expression plasmids for SRPK1 and SRPK2 were transfected into Huh7/Rep-Feo-1b cells or into HCV-JFH1-infected Huh7.5.1 cells. Forty-eight hours after transfection, cells were fixed and incubated with mouse anti-NS5A or anti-core antibodies and rabbit anti-HA antibody, followed by Alexa Fluor 488-labeled anti-mouse IgG and Alexa Fluor 568-labeled anti-rabbit IgG secondary antibodies. Nuclei were stained with DAPI. Representative immunofluorescence images derived from a number of experiments are shown as three images of a single focal plane of Huh7 cells, showing NS5A and core proteins (green), SRPK1 and SRPK2 (red), DAPI staining (blue), and the superimposed images (merge).

indicated that the SRPK inhibitor had specific suppressive effects on HCV subgenomic replication and that these effects are not due to cytotoxicity.

SRPIN340 suppresses HCV-JFH1 in cell culture. Next, we assessed the effects of the SRPK inhibitor on HCV-JFH1 in cell culture. Various concentrations of SRPIN340 were added to HCV-JFH1-infected Huh7 cells, and core antigen was quantified in the medium after 48 h of incubation. As shown in Fig. 4A, SRPIN340 significantly suppressed HCV core antigen secretion in a dose-dependent manner. An MTS-based cell viability assay did not show significant cytotoxicity from these inhibitors (Fig. 4B). In Western blotting, SRPIN340 suppressed expression of intracellular core protein by HCV-JFH1-infected cells in a dose-dependent manner; incubation with 30 μM SRPIN340 suppressed core protein expression by 54% of the drug-negative control, while SRPIN614 did not suppress core protein expression substantially (Fig. 4C). The effects of SRPIN340 on cellular HCV RNA were confirmed by real-time RT-PCR analyses (Fig. 4D). Similarly, in immunofluorescence microscopy, treatment with SRPIN340 resulted in a dose-dependent decrease in the number of HCV core-positive cells, but no effect was detected following treatment with SRPIN614 (Fig. 4E). These data indicate that SRPK inhibitors have antiviral effects on HCV infection and replication *in vitro*.

Overexpression and knockdown of SRPKs regulated HCV subgenomic replication. Next, we investigated the effects of the cellular expression levels of SRPK on HCV replication by overexpression and knockdown experiments. Expression plasmids for SRPK1 and SRPK2 were transfected individually into Huh7/Rep-Feo-1b cells, and internal luciferase activities were measured 72 h after transfection. The SRPK plasmid-transfected Huh7 cells expressed HA-tagged SRPK1 and SRPK2

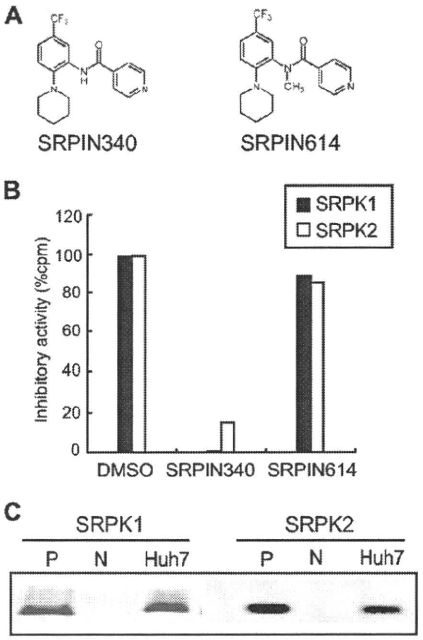

FIG. 2. Chemical structures and activities of SRPIN340 and SRPIN614. (A) Chemical structures of the SRPK inhibitor, SRPIN340, and activity-lacking control, SRPIN614. (B) Relative kinase activities of SRPK1 (black columns) and SRPK2 (white columns) *in vitro*, in the presence of the reagents indicated, SRPIN340, SRPIN614, and dimethyl sulfoxide (DMSO). (C) Expression of SRPK1 and SRPK2 mRNA by RT-PCR. P denotes positive controls, which are 1 ng of the respective SRPK expression plasmids. N denotes the template-lacking negative control.

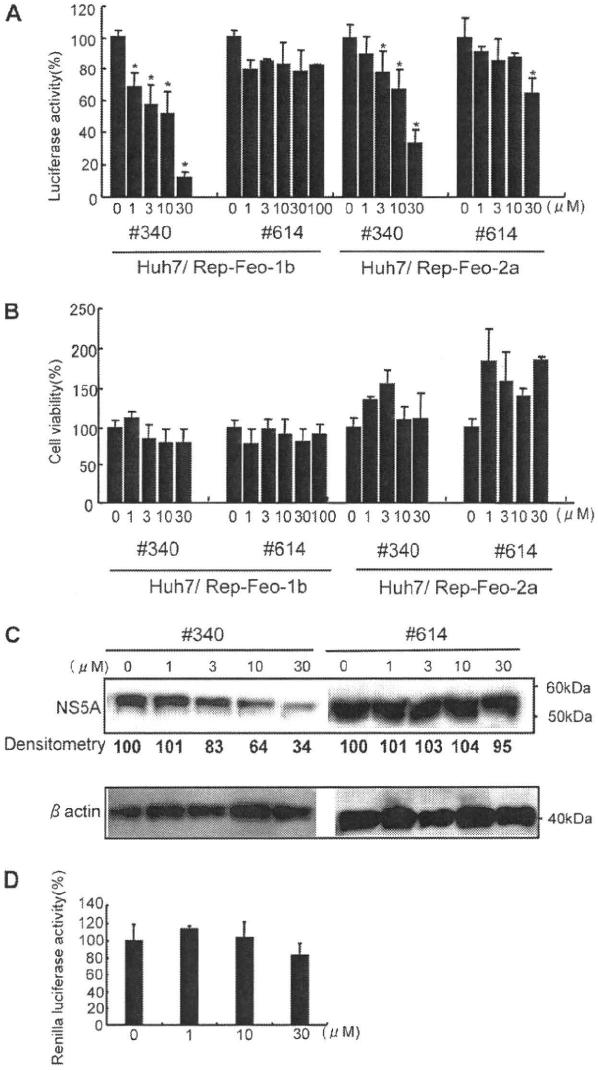

FIG. 3. Effects of SRPIN340 and SRPIN614 on expression of HCV subgenomic replicons. Huh7/Rep-Feo-1b or Huh7/Rep-Feo-2a cells were cultured in the presence of SRPIN340 (no. 340) or SRPIN614 (no. 614) at the concentrations indicated. After 48 h of culture, a luciferase assay (A), a cell viability assay (B), and Western blotting (C) were performed. (A) Effect of SRPIN340 and SRPIN614 on levels of HCV replication represented by replicon-dependent internal luciferase activities. Bars indicate luciferase activities relative to that of the drug-negative control. (B) Effect of SRPIN340 and SRPIN614 on cell viability. MTS assays were performed after culture in the presence of the drugs indicated. Bars indicate values relative to that of the drug-negative control. Asterisks indicate P values of less than 0.05. (C) Western blotting analyses. The expression levels of NS5A and beta-actin were detected by using anti-NS5A and anti-beta-actin antibodies. Densitometry of NS5A protein was performed, and results are indicated as percentages of the drug-negative control. The assay was repeated three times, and a representative result is shown. (D) Effect of SRPIN340 on EMCV-IRES-driven protein expression. Plasmid pECMV/IRES-Rluc was transfected into Huh7 cells. Twenty-four hours after transfection, the cells were incubated in indicated concentrations of SRPIN340. The renilla luciferase assay was performed at 48 h after incubation. In panels A, B, and D, assays were done in quadruplicate, and error bars indicate standard deviations.

proteins (Fig. 5A). Transfection efficiencies were ~20% in each experiment and were not different between expression plasmids. As shown in Fig. 5B, the luciferase activities were significantly increased in Huh7/Rep-Feo-1b cells transfected with SRPK1 or SRPK2. Western blotting showed that cellular expression of the HCV NS5A protein was increased in replicon-expressing cells with overexpression of SRPK1 or SRPK2 (Fig. 5C).

Four synthetic siRNAs were used to investigate the effects on HCV replication of suppression of expression of SRPK1 and SRPK2 proteins. These were directed against SRPK1 (siRNA 1 and siRNA 2) and SRPK2 (siRNA 3 and siRNA 4). Transgenic expression of SRPK1 and SRPK2 was specifically suppressed by transfection of the relevant siRNAs into Huh7 cells (Fig. 6A). Next, various amounts of individual siRNA (siRNA 1, 2, 3, or 4) were transfected into Huh7/Rep-Feo-1b cells, and luciferase assays were carried out 48 h after transfection. As shown in Fig. 6B, each siRNA suppressed expression of the HCV replicon. Western blotting also showed suppression of HCV protein expression after transfection of each siRNA (Fig. 6C). These results indicated that expression of SRPK1 and SRPK2 is positively correlated with the efficiency of HCV replication.

Absence of viral or cellular resistance to SRPIN340. In order to assess whether long-term exposure to the antiviral molecule could select a resistant replicon, we compared sensitivity to

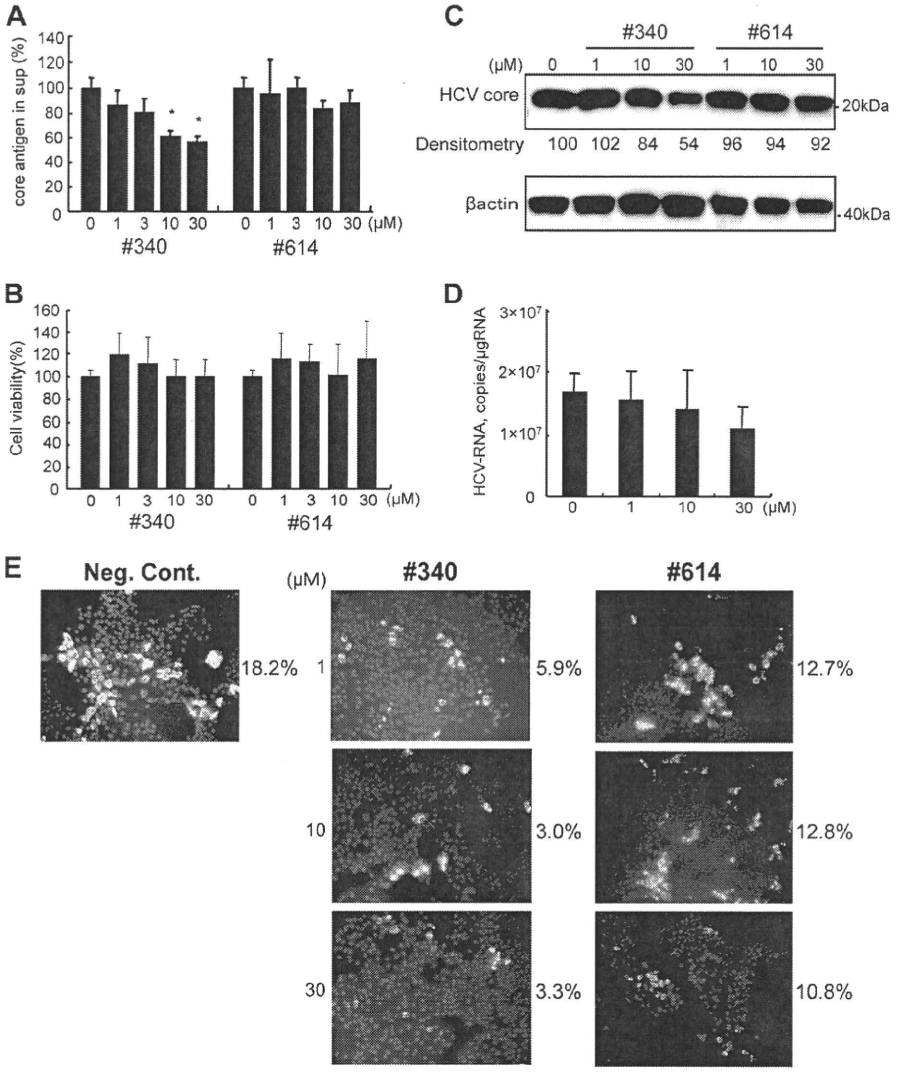

FIG. 4. Effect of SRPIN340 and SRPIN614 on HCV-JFH1 virus replication. HCV-JFH1-stably infected Huh7 cells of ~14 days were cultured in the presence of SRPIN340 or SRPIN614 at the concentrations indicated. After 48 h, cellular and supernatant HCV core antigens were detected. (A) HCV core antigen assays of culture supernatant (sup). Bars indicate values relative to that of the drug-negative control. Asterisks indicate *P* values of less than 0.05. (B) Effect of SRPIN340 and SRPIN614 on cell viability. MTS assays were performed 48 h after culture in the presence of the drugs indicated. Bars indicate values relative to that of the drug-negative control. (C) Western blotting analyses. The expression of HCV core and beta-actin was detected using anti-core and anti-beta-actin antibodies. Densitometry of HCV core protein was performed, and results are indicated as percentages of the drug-negative control. (D) Real-time RT-PCR analyses. Cells were harvested at 48 h after SRPIN340 treatment. (E) Immunofluorescence microscopy. Naïve Huh7.5.1 cells were infected with HCV-JFH1 culture supernatant at a multiplicity of infection of 0.1. Three days after infection, SRPK340 or SRPIN614 was added. After 48 h, cells were incubated with anti-core antibodies followed by Alexa Fluor-conjugated secondary antibody (green). Nuclei were stained with DAPI (blue). The percentages of HCV core-positive cells were calculated and are indicated on the right of each view. The assay was repeated three times, and a representative result is shown. Neg. cont., negative control. In panels A, B, and D, assays were done in triplicate, and error bars indicate standard deviations.

SRPIN340 between HCV replicon cells after continuous treatment of the drug and their control cells (Fig. 7A). Huh7/Rep-Feo-1b cells were treated with or without 30 μM SRPIN340 for 2 weeks. After 1 week of recovery culture without SRPIN340, a cell line, designated Huh7/Rep-Feo-1b(R), was established. As shown in Fig. 7B, the suppressive effect of SRPIN340 was not significantly different between Huh/Rep-Feo-1b(R) and its control cell line. These results suggest that SRPIN340 treatment under these conditions may not see the emergence of drug-resistant HCV replicons or cellular hyporesponsiveness to the drug.

DISCUSSION

These results demonstrate that small molecule inhibitors of cellular SRPK1 and SRPK2 (Fig. 2A) efficiently and specifically suppress intracellular replication of HCV subgenomic

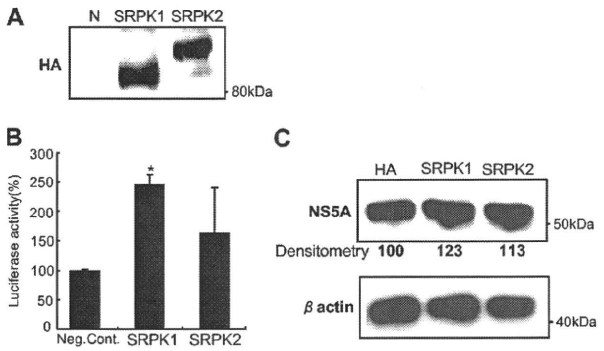

FIG. 5. Effects of overexpression of SRPK1 and SRPK2 on HCV replication. (A) The expression of transfected HA-tagged SRPK1 and SRPK2 was detected by anti-HA antibody. (B) Huh7/Rep-Feo-1b cells seeded on 24-well plates were transfected with 0.2 μg of expression plasmids for SRPK1 or SRPK2 or empty vector. Forty-eight hours after transfection, the levels of HCV replication were measured by luciferase assay. Bars indicate values relative to that of the empty vector-transfected control. Assays were done in triplicate, and error bars indicate standard deviations. Asterisks indicate *P* values of less than 0.05 compared with the control. (C) Expression of HCV NS5A and beta-actin was detected using anti-NS5A and anti-beta-actin antibodies. Densitometry of HCV core protein was performed, and results are indicated as percentages of the control.

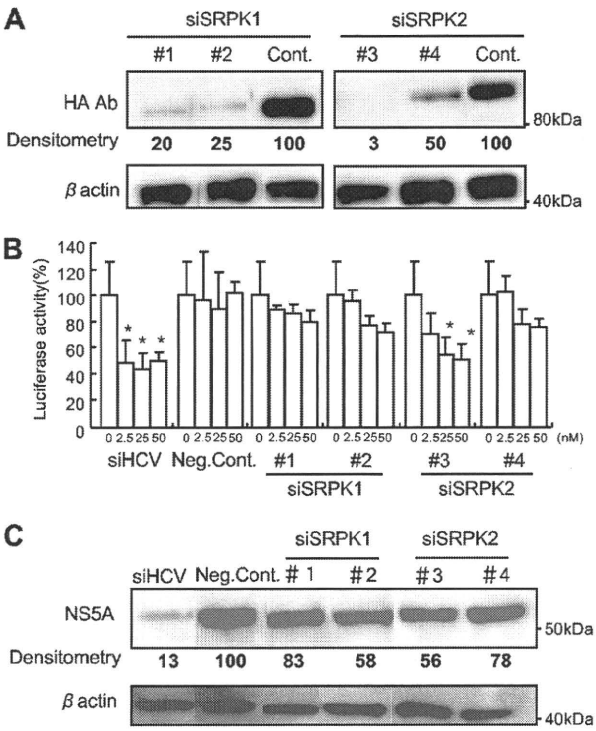

FIG. 6. Effects of siRNA knockdown of SRPK1 and SRPK2. (A) Huh7 cells were transfected with SRPK1 or SRPK2 expression plasmids and siRNA directed against SRPK1 (siSRPK1 no. 1 and siSRPK1 no. 2) or SRPK2 (siSRPK2 no. 3 and siSRPK2 no. 4) or control siRNA (32). Forty-eight hours after transfection, Western blotting was performed using anti-HA and anti-beta-actin antibodies. (B) Effects of siRNAs on HCV replication. The siRNAs indicated were transfected into Huh7/Rep-Feo-1b cells, and luciferase activities were measured 48 h after transfection. siHCV denotes the positive control, siRNA directed against the 5′-untranslated region of the HCV genome, and Neg. Cont. denotes a negative-control siRNA targeting an unrelated gene, which has been described previously (32). Bars indicate values relative to that of the mock-transfected control. Assays were done in triplicate, and error bars indicate standard deviations. Asterisks indicate *P* values of less than 0.05. (C) Western blotting analyses. Fifty micromoles of the siRNAs indicated was transfected into Huh7/Rep-Feo-1b cells. Forty-eight hours after transfection, cells were harvested and subjected to Western blotting. Expression of NS5A and beta-actin was detected with the relevant antibodies. Densitometry of NS5A protein was performed, and results are indicated as percentages of the control.

replicons and HCV-JFH1 viruses in cell culture, in a dose-dependent manner (Fig. 3 and 4). Real-time RT-PCR and Western blot analyses revealed that both RNA synthesis and its translation were reduced by SRPIN340. This inhibition was not associated with antiproliferative or nonspecific cytotoxic effects on the host cells (Fig. 3B and 4B). Transgenic overexpression of SRPK1 or SRPK2 resulted in augmentation of HCV replication and infection (Fig. 5). On the other hand, siRNA-mediated knockdown of these SRPKs suppressed HCV replication significantly (Fig. 6). These results demonstrate the dependence of the virus on the host RNA processing machinery that consists of SR proteins and their regulator, SRPK, and indicate that the inhibition of host SRPKs by small molecules may constitute a novel antiviral treatment against HCV.

SRPK1 and SRPK2 belong to the serine/threonine protein kinases. The two SRPKs efficiently phosphorylate SR proteins, such as the splicing factors ASF/SF2 and SC35, at their RS domains (3, 31). Overexpression of either SRPK1 or SRPK2 induces the phosphorylation-dependent shift of SR proteins from nuclear speckles to the nucleoplasm (8). Because SR proteins regulate splice site selection and spliceosome assembly, SRPK-mediated phosphorylation and cellular redistribution of SR proteins have been implicated in the control of mRNA maturation and alternative RNA splicing (31).

It remains to be clarified how the SRPK and SR proteins are involved in HCV replication and how the SRPIN340-directed suppression of such proteins leads to suppression of replication. There are several possibilities: that SRPIN340 may suppress processing of mRNAs that encode essential host proteins for HCV replication, that it suppresses alternative processing of the viral genomic RNA, and that certain viral proteins are substrates of host SRPK. Li et al. screened host factors required for HCV propagation through genome-wide siRNA targeting (17). They did not identify SRPKs as essential host proteins for HCV infection. Because our SRPIN340 inhibits both SRPK1 and SRPK2 and may target other family members of SRPK that possess the same target domain, it is still possible that the maintenance of overall SRPK activity may be essential for cellular HCV replication.

Several lines of evidence suggest that the viral life cycle may be partly governed by the regulation of SR protein phosphorylation as part of the RNA-processing machinery. It has been reported that virus infection induces dephosphorylation and functional inactivation of SR proteins. As a possible mechanism, Kanj et al. (13) have reported that adenoviral infection caused cellular accumulation of ceramide, which induces dephosphorylation of SR proteins by activation of the host pro-

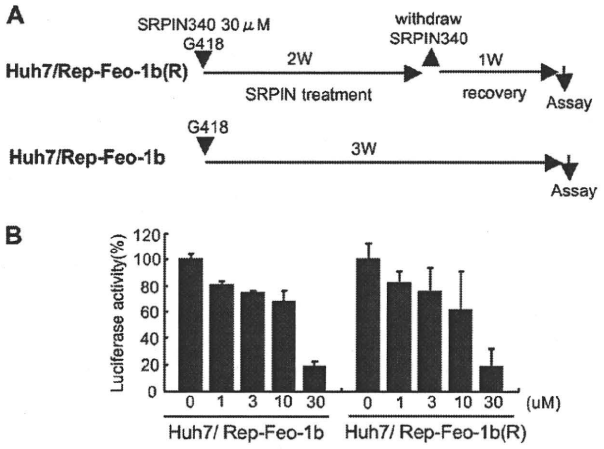

FIG. 7. Drug resistance assay of HCV replicon cells. (A) Schema for the establishment of SRPIN340-resistant cells and the control cells. Huh7/Rep-Feo-1b cells were treated with or without 30 μM SRPIN340 for 2 weeks in the presence of 500 μg/ml of G418. After 1 week of recovery culture without SRPIN340, a cell line, Huh7/Rep-Feo-1b(R), was established. (B) Huh/Rep-Feo-1b and Huh7/Rep-Feo-1b(R) cell lines were cultured in the presence of indicated concentrations of SRPIN340. Forty-eight hours after culture, internal luciferase assays were performed. Bars indicate luciferase activities relative to that of the drug-negative control. Assays were done in quadruplicate, and error bars indicate standard deviations.

tein phosphatase (PP)1 and consequently suppresses viral replication (2). At an early stage of adenoviral infection, the viral E4-ORF4 protein binds to the host PP2A and SR proteins, resulting in dephosphorylation of the SR proteins and consequent activation of IIIa splicing of the viral precursor mRNA that is the dominant transcript of the late phase of infection (5). In HIV infection, the role of SR proteins in the splicing of the proviral RNA has been demonstrated by a report that overexpression of SRp40, SRp55, or SRp75 caused overproduction of HIV (7). HIV Tat controls subcellular localization of SR proteins and establishes efficient HIV replication. These findings suggest that the levels of SR protein phosphorylation are positively correlated with early viral replication in host cells and that SRPIN340 treatment suppresses viral replication at an early stage.

It has been reported that HBV core protein is a substrate of SRPK1- and SRPK2-mediated phosphorylation (4). Phosphorylation of RS domains in HBV core prevents nonspecific RNA binding, which facilitates specific interaction of HBV core with the pregenomic RNA and formation of immature capsids. A functional similarity between HBV core protein and SR proteins has been reported. Our preliminary results showed that SRPIN340 suppressed expression of the viral proteins and secretion of HBe and HBs antigens. While we have not demonstrated SRPK-mediated phosphorylation of HCV proteins, our immunofluorescence microscopy has demonstrated partial colocalization of SRPKs and HCV NS5A and core proteins. These findings may suggest a possible direct interaction between SRPKs and HCV proteins, and those interactions may be the targets of SRPIN340.

Given the current situation of limited therapeutic options against HCV, searching for more potent and less toxic antiviral drugs is needed to improve clinical anti-HCV chemotherapeutics. Several direct antiviral agents against HCV are currently undergoing clinical trials; these include NS3 protease inhibitors and NS5B polymerase inhibitors (28). However, the frequent emergence of drug-resistant mutant viruses is a major weakness of such agents (15). Because our compound, SRPIN340, targets host proteins, it may be effective against multiple HCV genotypes and it is less likely that drug-resistant viruses will emerge (20). Furthermore, the toxicity data available for SRPIN340 are promising (7). No adverse effects were observed when SRPIN340 was administered orally to rats, even at the highest dose (2,000 mg/kg of body weight) for 2 weeks (data not shown). These data support the feasibility of long-term *in vivo* use of this compound to suppress HCV replication. On the other hand, the fact that this inhibitor acts through cellular components still raises concerns regarding its safety in the case of human use. We should not be reassured by the cytotoxicity data and the small-animal data, and further preclinical studies should be planned to address this issue. Overall, our results indicate that SRPIN340, which suppresses a wide range of DNA and RNA viruses, also is effective at suppressing HCV infection and replication. Future studies with SRPIN340, its derivatives, and other chemicals that target SRPKs could be directed toward developing a new class of antiviral treatment regimens and drugs.

ACKNOWLEDGMENTS

We thank Frank Chisari for providing Huh7.5.1 cells.

This study was supported by grants from Ministry of Education, Culture, Sports, Science and Technology—Japan, the Japan Society for the Promotion of Science, Research on Hepatitis and BSE, and Intractable Diseases, Ministry of Health, Labor and Welfare-Japan, Japan Health Sciences Foundation, and the National Institute of Biomedical Innovation.

We declare that we have nothing to disclose regarding funding from industries or conflicts of interest with respect to the study.

REFERENCES

1. **Alter, M. J.** 1997. Epidemiology of hepatitis C. Hepatology **26:**62S–65S.
2. **Chalfant, C. E., B. Ogretmen, S. Galadari, B. J. Kroesen, B. J. Pettus, and Y. A. Hannun.** 2001. FAS activation induces dephosphorylation of SR proteins; dependence on the de novo generation of ceramide and activation of protein phosphatase 1. J. Biol. Chem. **276:**44848–44855.
3. **Colwill, K., L. L. Feng, J. M. Yeakley, G. D. Gish, J. F. Caceres, T. Pawson, and X. D. Fu.** 1996. SRPK1 and Clk/Sty protein kinases show distinct substrate specificities for serine/arginine-rich splicing factors. J. Biol. Chem. **271:**24569–24575.
4. **Daub, H., S. Blencke, P. Habenberger, A. Kurtenbach, J. Dennenmoser, J. Wissing, A. Ullrich, and M. Cotten.** 2002. Identification of SRPK1 and SRPK2 as the major cellular protein kinases phosphorylating hepatitis B virus core protein. J. Virol. **76:**8124–8137.
5. **Estmer Nilsson, C., S. Petersen-Mahrt, C. Durot, R. Shtrichman, A. R. Krainer, T. Kleinberger, and G. Akusjarvi.** 2001. The adenovirus E4-ORF4 splicing enhancer protein interacts with a subset of phosphorylated SR proteins. EMBO J. **20:**864–871.
6. **Fried, M. W., M. L. Shiffman, K. R. Reddy, C. Smith, G. Marionos, F. L. Goncales, D. Häussinger, M. Diago, G. Garosi, D. Dhumeaux, A. Craxi, A. Lin, J. Hoffman, and J. Yu.** 2002. Peginterferon alfa-2a plus ribavirin for chronic hepatitis C virus infection. N. Engl. J. Med. **347:**975–982.
7. **Fukuhara, T., T. Hosoya, S. Shimizu, K. Sumi, T. Oshiro, Y. Yoshinaka, M. Suzuki, N. Yamamoto, L. A. Herzenberg, and M. Hagiwara.** 2006. Utilization of host SR protein kinases and RNA-splicing machinery during viral replication. Proc. Natl. Acad. Sci. U. S. A. **103:**11329–11333.
8. **Gui, J. F., W. S. Lane, and X. D. Fu.** 1994. A serine kinase regulates intracellular localization of splicing factors in the cell cycle. Nature **369:**678–682.
9. **Gui, J. F., H. Tronchere, S. D. Chandler, and X. D. Fu.** 1994. Purification and characterization of a kinase specific for the serine- and arginine-rich pre-mRNA splicing factors. Proc. Natl. Acad. Sci. U. S. A. **91:**10824–10828.
10. **Guo, J. T., V. V. Bichko, and C. Seeger.** 2001. Effect of alpha interferon on the hepatitis C virus replicon. J. Virol. **75:**8516–8523.

11. **Itsui, Y., N. Sakamoto, S. Kakinuma, M. Nakagawa, Y. Sekine-Osajima, M. Tasaka-Fujita, Y. Nishimura-Sakurai, G. Suda, Y. Karakama, M. Yamamoto, T. Watanabe, M. Ueyama, Y. Funaoka, S. Azuma, and M. Watanabe.** Antiviral effects of the interferon-induced protein GBP-1 and its interaction with the hepatitis C virus NS5B protein. Hepatology, in press.
12. **Itsui, Y., N. Sakamoto, M. Kurosaki, N. Kanazawa, Y. Tanabe, T. Koyama, Y. Takeda, M. Nakagawa, S. Kakinuma, Y. Sekine, S. Maekawa, N. Enomoto, and M. Watanabe.** 2006. Expressional screening of interferon-stimulated genes for antiviral activity against hepatitis C virus replication. J. Viral Hepat. **13:**690–700.
13. **Kanj, S. S., N. Dandashi, A. El-Hed, H. Harik, M. Maalouf, L. Kozhaya, T. Mousallem, A. E. Tollefson, W. S. Wold, C. E. Chalfant, and G. S. Dbaibo.** 2006. Ceramide regulates SR protein phosphorylation during adenoviral infection. Virology **345:**280–289.
14. **Kato, T., T. Date, M. Miyamoto, A. Furusaka, K. Tokushige, M. Mizokami, and T. Wakita.** 2003. Efficient replication of the genotype 2a hepatitis C virus subgenomic replicon. Gastroenterology **125:**1808–1817.
15. **Kuntzen, T., J. Timm, A. Berical, N. Lennon, A. M. Berlin, S. K. Young, B. Lee, D. Heckerman, J. Carlson, L. L. Reyor, M. Kleyman, C. M. McMahon, C. Birch, J. Schulze Zur Wiesch, T. Ledlie, M. Koehrsen, C. Kodira, A. D. Roberts, G. M. Lauer, H. R. Rosen, F. Bihl, A. Cerny, U. Spengler, Z. Liu, A. Y. Kim, Y. Xing, A. Schneidewind, M. A. Madey, J. F. Fleckenstein, V. M. Park, J. E. Galagan, C. Nusbaum, B. D. Walker, G. V. Lake-Bakaar, E. S. Daar, I. M. Jacobson, E. D. Gomperts, B. R. Edlin, S. M. Donfield, R. T. Chung, A. H. Talal, T. Marion, B. W. Birren, M. R. Henn, and T. M. Allen.** 2008. Naturally occurring dominant resistance mutations to hepatitis C virus protease and polymerase inhibitors in treatment-naive patients. Hepatology **48:**1769–1778.
16. **Kuroyanagi, N., H. Onogi, T. Wakabayashi, and M. Hagiwara.** 1998. Novel SR-protein-specific kinase, SRPK2, disassembles nuclear speckles. Biochem. Biophys. Res. Commun. **242:**357–364.
17. **Li, Q., A. L. Brass, A. Ng, Z. Hu, R. J. Xavier, T. J. Liang, and S. J. Elledge.** 2009. A genome-wide genetic screen for host factors required for hepatitis C virus propagation. Proc. Natl. Acad. Sci. U. S. A. **106:**16410–16415.
18. **Muraki, M., B. Ohkawara, T. Hosoya, H. Onogi, J. Koizumi, T. Koizumi, K. Sumi, J. Yomoda, M. V. Murray, H. Kimura, K. Furuichi, H. Shibuya, A. R. Krainer, M. Suzuki, and M. Hagiwara.** 2004. Manipulation of alternative splicing by a newly developed inhibitor of Clks. J. Biol. Chem. **279:**24246–24254.
19. **Nakagawa, M., N. Sakamoto, N. Enomoto, Y. Tanabe, N. Kanazawa, T. Koyama, M. Kurosaki, S. Maekawa, T. Yamashiro, C. H. Chen, Y. Itsui, S. Kakinuma, and M. Watanabe.** 2004. Specific inhibition of hepatitis C virus replication by cyclosporin A. Biochem. Biophys. Res. Commun. **313:**42–47.
20. **Nakagawa, M., N. Sakamoto, Y. Tanabe, T. Koyama, Y. Itsui, Y. Takeda, C. H. Chen, S. Kakinuma, S. Oooka, S. Maekawa, N. Enomoto, and M. Watanabe.** 2005. Suppression of hepatitis C virus replication by cyclosporin a is mediated by blockade of cyclophilins. Gastroenterology **129:**1031–1041.
21. **Ngo, J. C., S. Chakrabarti, J. H. Ding, A. Velazquez-Dones, B. Nolen, B. E. Aubol, J. A. Adams, X. D. Fu, and G. Ghosh.** 2005. Interplay between SRPK and Clk/Sty kinases in phosphorylation of the splicing factor ASF/SF2 is regulated by a docking motif in ASF/SF2. Mol. Cell **20:**77–89.
22. **Nishimura-Sakurai, Y., N. Sakamoto, K. Mogushi, S. Nagaie, M. Nakagawa, Y. Itsui, Y. Sekine-Osajima, M. Tasaka-Fujita, Y. Onuki-Karakama, G. Suda, K. Mishima, M. Yamamoto, M. Ueyama, Y. Funaoka, T. Watanabe, S. Azuma, S. Kakinuma, K. Tsuchiya, H. Tanaka, N. Enomoto, and M. Watanabe.** 2010. Comparison of HCV-associated gene expression and cell signaling pathways in cells with or without HCV replicon and in replicon-cured cells. J. Gastroenterol. **45:**523–536.
23. **Sakamoto, N., and M. Watanabe.** 2009. New therapeutic approaches to hepatitis C virus. J. Gastroenterol. **44:**643–649.
24. **Sakamoto, N., M. Yoshimura, T. Kimura, K. Toyama, Y. Sekine-Osajima, M. Watanabe, and M. Muramatsu.** 2007. Bone morphogenetic protein-7 and interferon-alpha synergistically suppress hepatitis C virus replicon. Biochem. Biophys. Res. Commun. **357:**467–473.
25. **Sciabica, K. S., Q. J. Dai, and R. M. Sandri-Goldin.** 2003. ICP27 interacts with SRPK1 to mediate HSV splicing inhibition by altering SR protein phosphorylation. EMBO J. **22:**1608–1619.
26. **Sekine-Osajima, Y., N. Sakamoto, K. Mishima, M. Nakagawa, Y. Itsui, M. Tasaka, Y. Nishimura-Sakurai, C. H. Chen, T. Kanai, K. Tsuchiya, T. Wakita, N. Enomoto, and M. Watanabe.** 2008. Development of plaque assays for hepatitis C virus-JFH1 strain and isolation of mutants with enhanced cytopathogenicity and replication capacity. Virology **371:**71–85.
27. **Tanabe, Y., N. Sakamoto, N. Enomoto, M. Kurosaki, E. Ueda, S. Maekawa, T. Yamashiro, M. Nakagawa, C. H. Chen, N. Kanazawa, and M. Watanabe.** 2004. Synergistic inhibition of intracellular hepatitis C virus replication by combination of ribavirin and interferon-alpha. J. Infect. Dis. **189:**1129–1139.
28. **Thompson, A. J., and J. G. McHutchison.** 2009. Antiviral resistance and specifically targeted therapy for HCV (STAT-C). J. Viral Hepat. **16:**377–387.
29. **Valcarcel, J., and M. R. Green.** 1996. The SR protein family: pleiotropic functions in pre-mRNA splicing. Trends Biochem. Sci. **21:**296–301.
30. **Wakita, T., T. Pietschmann, T. Kato, T. Date, M. Miyamoto, Z. Zhao, K. Murthy, A. Habermann, H. G. Krausslich, M. Mizokami, R. Bartenschlager, and T. J. Liang.** 2005. Production of infectious hepatitis C virus in tissue culture from a cloned viral genome. Nat. Med. **11:**791–796.
31. **Wang, H. Y., W. Lin, J. A. Dyck, J. M. Yeakley, Z. Songyang, L. C. Cantley, and X. D. Fu.** 1998. SRPK2: a differentially expressed SR protein-specific kinase involved in mediating the interaction and localization of pre-mRNA splicing factors in mammalian cells. J. Cell Biol. **140:**737–750.
32. **Yokota, T., N. Sakamoto, N. Enomoto, Y. Tanabe, M. Miyagishi, S. Maekawa, L. Yi, M. Kurosaki, K. Taira, M. Watanabe, and H. Mizusawa.** 2003. Inhibition of intracellular hepatitis C virus replication by synthetic and vector-derived small interfering RNAs. EMBO Rep. **4:**602–608.
33. **Zheng, Y., X. D. Fu, and J. H. Ou.** 2005. Suppression of hepatitis B virus replication by SRPK1 and SRPK2 via a pathway independent of the phosphorylation of the viral core protein. Virology **342:**150–158.
34. **Zhong, J., P. Gastaminza, G. Cheng, S. Kapadia, T. Kato, D. R. Burton, S. F. Wieland, S. L. Uprichard, T. Wakita, and F. V. Chisari.** 2005. Robust hepatitis C virus infection in vitro. Proc. Natl. Acad. Sci. U. S. A. **102:**9294–9299.

Organic & Biomolecular Chemistry

www.rsc.org/obc

Volume 8 | Number 18 | 21 September 2010 | Pages 4029–4184

ISSN 1477-0520

RSC Publishing

Strain-promoted double-click reaction for chemical modification of azido-biomolecules†

Isao Kii,*[a] Akira Shiraishi,[a] Toshiyuki Hiramatsu,[a,b] Takeshi Matsushita,[c] Hidehiro Uekusa,[d] Suguru Yoshida,[b] Makoto Yamamoto,[e] Akira Kudo,[a] Masatoshi Hagiwara[e] and Takamitsu Hosoya*[a,b]

Received 15th April 2010, Accepted 8th July 2010
First published as an Advance Article on the web 26th July 2010
DOI: 10.1039/c0ob00003e

The strain-promoted "double-click" (SPDC) reaction using Sondheimer diyne, a novel convergent method conjugating three molecules spontaneously, has enabled us to readily modify an azido-biomolecule with a small reporter azido-molecule.

"Click reaction," copper(I)-catalyzed azide–alkyne [3+2] cycloaddition (CuAAC), is an emerging method for conjugating molecules in the fields of chemistry and biology.[1–3] With the progress in preparation techniques of biomolecules incorporated with bioorthogonal groups, various chemically-modified biomolecules have become available.[4] However, cytotoxicity by the copper catalyst and the slow rate of the reaction have restricted its application. To overcome these limitations, Bertozzi has introduced a copper-free click reaction, the strain-promoted azide–alkyne [3+2] cycloaddition (SPAAC),[5] exploiting the spontaneous reactivity of cyclooctynes toward an azide by its ring strain.[6] Furthermore, a rapid SPAAC reaction has been achieved using difluorinated cyclooctyne (DIFO, **1**),[7] dibenzocyclooctynol (DIBO, **2a**)[8] and aza-dibenzocyclooctyne (DIBAC, **2b**;[9] BARAC, **2c**[7f]) derivatives. Fluorescence-labeled or biotinylated derivatives of these cyclooctynes have enabled us to visualize the distribution of azido-glycoconjugates in cultured cells and in living animals.[7,8]

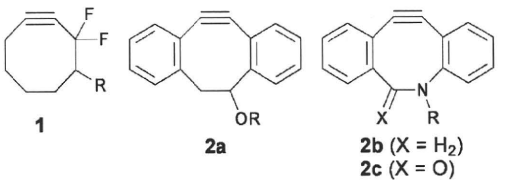

1 **2a** **2b** (X = H_2) **2c** (X = O)

To expand the versatility of the SPAAC reaction, we have conceived the idea of connecting two azides by a bisreactive molecule, thereby avoiding the on-demand preparation of cyclooctyne derivatives. We envisaged that *sym*-dibenzo-1,5-cyclooctadiene-3,7-diyne (**3**), reported by Sondheimer[10] and now easily available,[11] is an ideal compound because it has two highly strained alkyne bonds[12] ready to react spontaneously.[13] Herein, we show the catalyst-free dual annulation of diyne **3** with two different azido-molecules, the strain-promoted "double-click" (SPDC) reaction (Scheme 1), and demonstrate the chemical modification of an azido-biomolecule with a reporter azido-molecule in both *in vitro* and living cells.

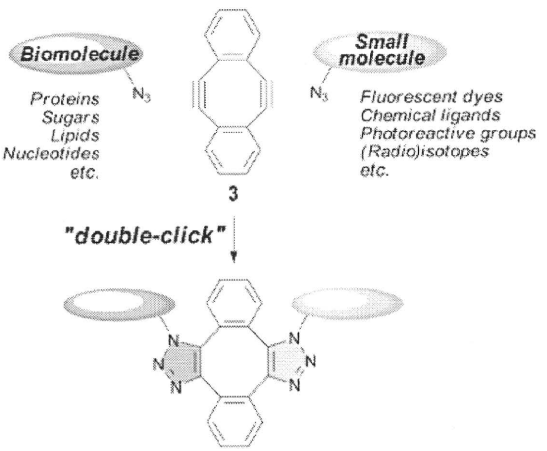

Scheme 1 Chemical modification of azido-biomolecules with small azido-molecules by the strain-promoted double-click (SPDC) reaction.

In an initial study, diyne **3** in methanol (8 mM) was treated with an excess amount of benzyl azide (**4a**, 2.4 equiv.) at room temperature (Scheme 2, R = benzyl). After 70 min, diyne **3** completely reacted to give two regioisomeric bis-cycloadducts **6a** (*trans*) and **7a** (*cis*) in 60% and 38% yields, respectively.[14] X-Ray crystallographic analysis showed their unique saddle-shaped structures (Fig. 1).[15] The mono-cycloadduct **5a**, the presumed monoyne intermediate, was neither isolated nor detected even when an equimolar amount of **4a** was used,[14] indicating that the monoyne intermediate is more reactive toward azides than the starting diyne **3**.

The broad substrate scope in the SPDC reaction was shown from the reactions of diyne **3** with various azides, including ethyl azidoacetate (**4b**), phenyl azide (**4c**), 4-(azidomethyl)benzyl alcohol (**4d**) and methyl 4-(azidomethyl)benzoate (**4e**) (Scheme 2).[14–16] Not surprisingly, the reaction of diyne **3** with an equimolar mixture

[a]*Department of Biological Information, Graduate School of Bioscience and Biotechnology, Tokyo Institute of Technology, 4259 Nagatsuta-cho, Midori-ku, Yokohama 226-8501, Japan. E-mail: ikii@bio.titech.ac.jp*
[b]*Laboratory of Chemical Biology, Graduate School of Biomedical Science, Institute of Biomaterials and Bioengineering, Tokyo Medical and Dental University and SORST, Japan Science and Technology Agency (JST), 2-3-10 Kanda-Surugadai, Chiyoda-ku, Tokyo 101-0062, Japan. E-mail: thosoya.cb@tmd.ac.jp; Fax: +81-3-5280-8117*
[c]*Goi Research Center, Chisso Petrochemical Corporation, 5-1 Goikaigan, Ichihara, Chiba 290-8551, Japan*
[d]*Department of Chemistry and Materials Science, Graduate School of Science and Engineering, Tokyo Institute of Technology, 2-12-1 Ookayama, Meguro-ku, Tokyo, 152-8551, Japan*
[e]*Department of Functional Genomics, Medical Research Institute, Graduate School of Biomedical Science, Tokyo Medical and Dental University, 1-5-45 Yushima, Bunkyo-ku, Tokyo 113-8510, Japan*

† Electronic supplementary information (ESI) available: Experimental details for syntheses and characterization of new compounds, kinetic study, computational studies and biological experiments. See DOI: 10.1039/c0ob00003e

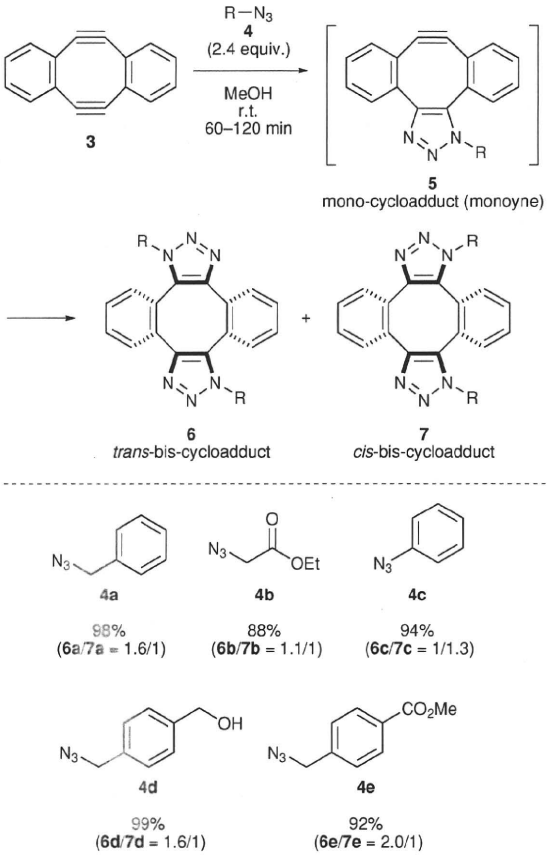

Scheme 2 SPDC reaction of diyne **3** with various azides.

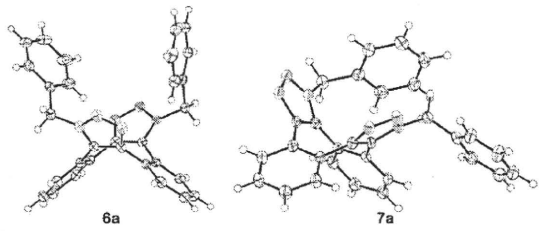

Fig. 1 Structures of bis-cycloadducts **6a** (CCDC 759900) and **7a** (CCDC 759902).

of two different azides gave regioisomeric hetero-cycloadducts as the major products and two pairs of homo-cycloadducts. For example, the reaction of **3** with 1.2 equiv. each of **4d** and **4e** gave regioisomeric heterocycloadducts in 43% combined yield (*trans*/*cis* = 1.2/1), along with homocycloadducts **6d**/**7d** (1.8/1) and **6e**/**7e** (1.2/1) in 28% and 27% yields, respectively.[14]

Fig. 2 shows the computation on the activation barriers and transition states of the SPDC reaction of diyne **3** with methyl azide (**4f**) by a density functional theory (DFT) method.[14,17] The barriers for all cycloadditions were low, confirming the spontaneous reaction of both diyne **3** and monoyne **5f** with **4f** at room temperature. Notably, the activation energy of the second cycloaddition was smaller (+8.8 and +9.5 kcal mol^{-1} for *trans*- and *cis*-adducts, respectively) than that of the first cycloaddition (+12.4

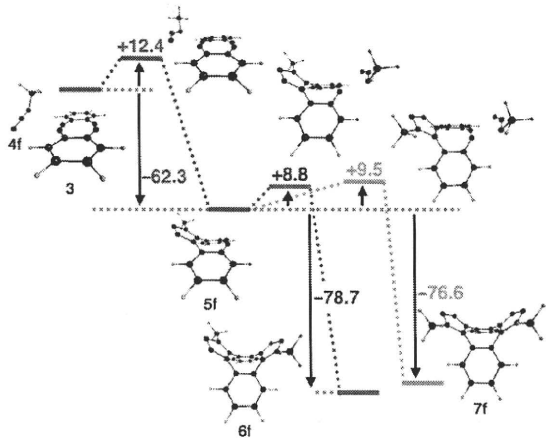

Fig. 2 Potential energy diagram of the SPDC reaction using the B3LYP/6-31G(d) DFT method, showing the relevant stationary points and transition states on the potential energy surfaces for each cycloaddition. All energies (kcal mol^{-1}) include zero-point energy corrections at the level used for geometry optimization.

kcal mol^{-1}), supporting the higher reactivity of the monoyne intermediate.[18] The Kohn–Sham HOMO and LUMO orbital surfaces of each transition states also confirmed the high reactivity of **5f**.[14] The higher reactivity of the monoyne intermediate than the diyne can be attributed to its highly-distorted alkyne bond, which likely arose from the steric repulsion between the substituent on the triazole ring and hydrogen atom on the benzene ring.

To examine the feasibility of chemical modification of azido-biomolecules by the SPDC reaction, we planned to modify an azido-incorporated protein. Among the several methods to prepare azido-proteins,[19,20] we chose to use HaloTag protein that binds covalently with HaloTag ligand possessing a long-chain chloroalkane.[21] The reaction of azido-HaloTag ligand **8** with GST-fused HaloTag protein bound on the GSH-Sepharose resin (HaloTag-GST-resin) gave the desired azido-HaloTag-GST-resin. The fluorescence modification of the azido-HaloTag-GST-resin by the SPDC reaction was attempted by adding diyne **3** into a solution containing azido-HaloTag-GST-resin and TESRA-PEO_3-azide (**9**), an azido-conjugated tetraethylsulforhodamine (TESRA) derivative (Fig. 3(a)). SDS-PAGE analysis showed the fluorescent band (51 kDa) that corresponds to the TESRA-labeled HaloTag-GST protein with nearly 40% of total labeling efficiency (Fig. 3(b), lane 3).[22,23]

Unexpectedly, a sequential procedure, treating azido-HaloTag-GST-resin with **3** and then adding **9** after quick washing out of unreacted **3** by buffer, also achieved the fluorescence labeling of the azido-HaloTag-GST protein with approximately 45% efficiency (Fig. 3(b), lane 7). Under these conditions, the signal for the homo-dimer of the azido-HaloTag-GST protein was substantially undetected.[14] Furthermore, the dimerized product was also hard to detect even in the SPDC modification of soluble azido-HaloTag protein that was free from the resin,[14] indicating that the SPDC reaction between the azido-proteins is not easy to proceed. These results suggest that the monoyne intermediate has a certain lifetime during SPDC reaction under the biological experimental conditions and is available for rapid SPAAC reaction with a different azido-molecule. The noticeable difference between the

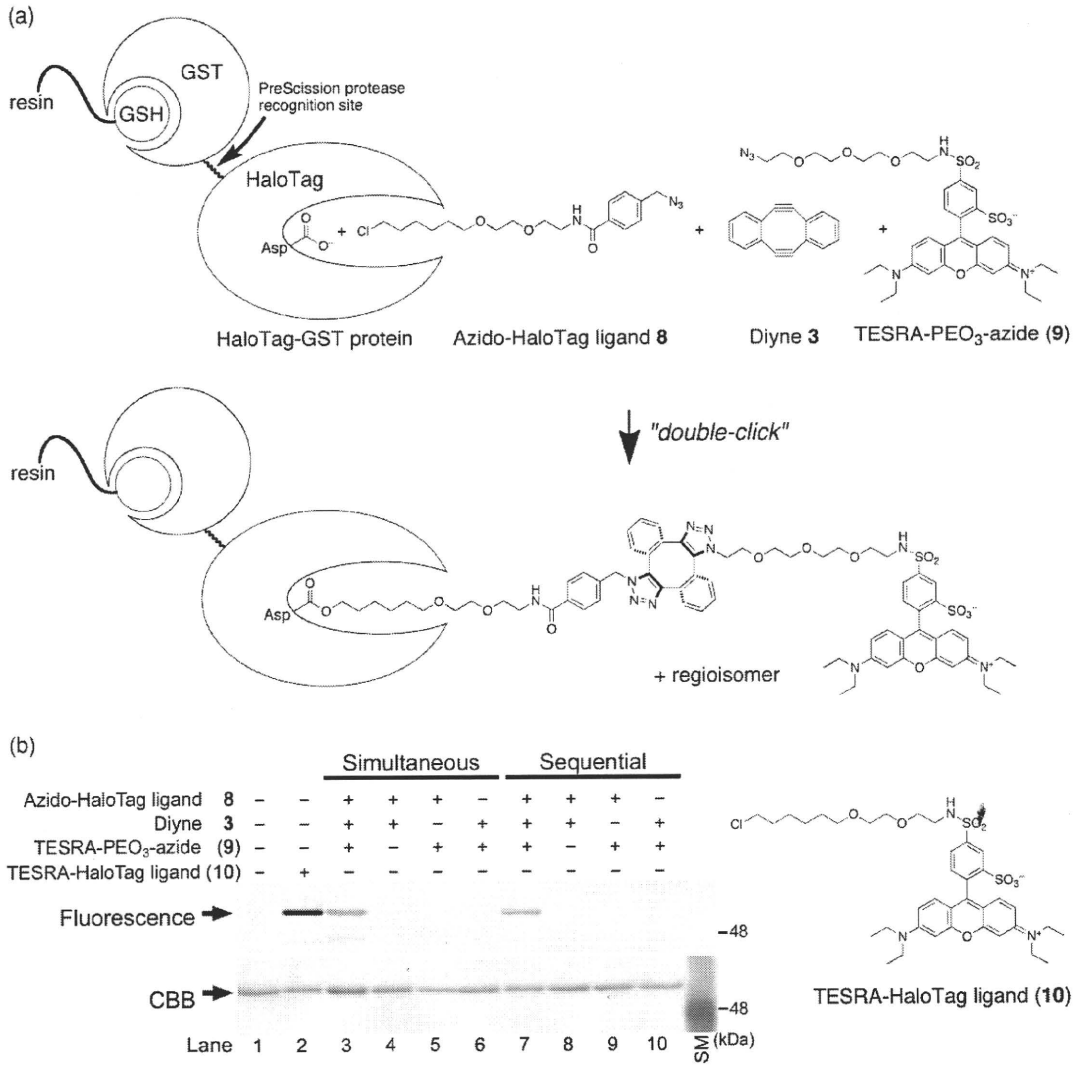

Fig. 3 (a) Schematic view of the SPDC modification of azido-incorporated HaloTag-GST bound on the resin with TESRA-PEO_3-azide (**9**) using diyne **3**. HaloTag protein is a modified haloalkane dehalogenase designed to bind covalently with a specific synthetic ligand, so-called HaloTag ligand bearing a long chloroalkane chain.[21] The chloroalkyl moiety of HaloTag ligand inserts into a binding pocket of HaloTag protein and S_N2 reaction occurs on asparatic acid residue of the protein to form an ester bond. The recognition of the ligands by HaloTag protein is highly specific, ester bond formation occurs rapidly under physiological conditions, and is essentially irreversible. The HaloTag protein was produced in *E. coli* as a glutathione *S*-transferase (GST) tag fusion protein (HaloTag-GST protein), in which a cleavage site recognized by PreScission protease was located between the tags. The HaloTag-GST protein bound on the GSH-Sepharose resin (HaloTag-GST-resin) was incubated with azido-HaloTag ligand **8** to give azido-incorporated HaloTag-GST protein bound on the resin (azido-HaloTag-GST-resin). The azido-HaloTag-GST-resin was incubated with diyne **3** and TESRA-PEO_3-azide (**9**) (simultaneous modification), or with **3** followed by with **9** (sequential modification). The labeled protein was subjected to SDS-PAGE analysis after elution from the GSH-Sepharose resin (b) or to MALDI-TOF-MS analysis after proteolytic excision between GST and HaloTag protein by PreScission protease.[22] (b) SDS-PAGE analysis of GST-fused HaloTag protein eluted from the resin. Purified HaloTag-GST-resin was treated with buffer (–) or azido-HaloTag ligand **8** (100 μM) overnight at 4 °C. The azido-HaloTag-GST-resin was incubated with buffer (–) or diyne **3** (200 μM), and buffer (–) or TESRA-PEO_3-azide (**9**) (200 μM) in the same tube for 15 min at r.t. (Lanes 3–6; simultaneous procedure). The azido-HaloTag-GST-resin was also treated with buffer (–) or **3** for 15 min at r.t., quickly washed with buffer, and then treated with buffer (–) or **9** for 10 min at r.t. (Lanes 7–10; sequential procedure). As a positive control, HaloTag-GST-resin was reacted with TESRA-HaloTag ligand (**10**) (100 μM) overnight at 4 °C (Lane 2). The proteins on the resin were eluted by incubation with SDS-sample buffer containing 10 mM DTT for 5 min at 100 °C, and then subjected to SDS-PAGE. The gel was scanned with a fluorescence image analyzer (Typhoon 8600) and then stained with Coomassie brilliant blue (CBB). SM indicates size marker.

SPDC modification of the azido-protein and the SPDC reaction in an organic solvent, in which the monoyne intermediate could not be detected, can be attributed to the different reaction conditions. The former was performed using ~20 μM of the azido-protein in the presence of excess amounts of diyne **3**, whereas the latter was carried out with ~20 mM of small azido compound

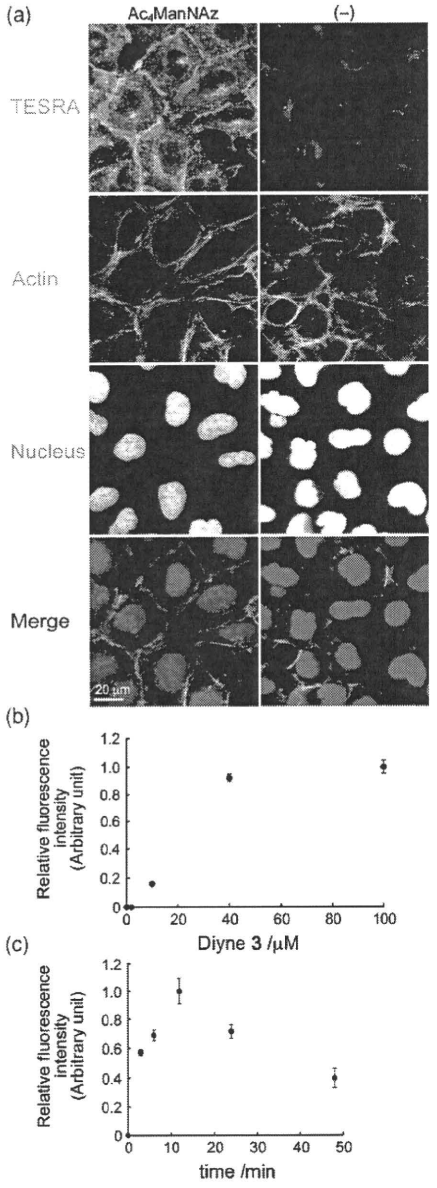

Fig. 4 Cell-surface labeling with diyne **3** and TESRA-PEO_3-azide (**9**). HEK293 cells were incubated for 2 days in the absence (–) or presence of Ac_4ManNAz (100 μM). (a) The azidosugar-incorporated cells were incubated with **3** (40 μM) for 20 min at 37 °C, quickly rinsed with buffer, and then treated with **9** (40 μM) for 20 min at 37 °C. The labeled cells were fixed, and then stained with Alexa Fluor 488-conjugated phalloidin and TO-PRO-3 to visualize cytoskeletal actin fibers and nuclei, respectively. (b) The azidosugar-incorporated cells were incubated with **3** (0 to 100 μM) for 20 min at 37 °C, quickly rinsed, and then treated with **9** (40 μM) for 20 min at 37 °C. Relative fluorescence intensity was determined by densitometric analysis of the fluorescence images. (c) The azidosugar-incorporated cells were incubated with **3** (40 μM) for various times (0 to 48 min) at 37 °C, quickly rinsed, then treated with **9** (40 μM) for 20 min at 37 °C, and analyzed as in (b).

toward 8 mM of diyne **3**. Thus, the dilute condition as well as the lower mobility of the protein would largely reduce the frequency of coming close to each other and prevent the dimerization of azido-proteins.

In order to apply the SPDC modification in living cells, we examined fluorescence labeling of azido-glycoconjugates on the cell surface. HEK293 cells, cultured with a medium containing tetraacetylated *N*-azidoacetyl-D-mannosamine (Ac_4ManNAz),[24] was incubated with diyne **3** and, after quick rinsing with buffer to remove unreacted **3**, TESRA-PEO_3-azide (**9**) was added. Consequently, the azidosugar-incorporated cells exhibited reliable fluorescent signals in the boundary between the cells (Fig. 4(a), left panels), marking a sharp contrast with the control cells which showed negligible signals (Fig. 4(a), right panels). Optimal results were obtained using diyne **3** at the concentrations of 40 to 100 μM (Fig. 4(b)).[25] Maximum labeling efficiency was achieved by treating **3** (40 μM) within 20 min (Fig. 4(c)). Long-time incubation reduced the labeling efficiency (Fig. 4(c)), indicating the time-dependent degradation of the highly reactive monoyne intermediate. The commercially available Alexa Fluor 488 azide was also used in both sequential and simultaneous procedures.[14]

Furthermore, the SPDC modification of azido-glycoconjugates with **3** and a fluorescein-conjugated azide showed a comparable result to that of the single-click modification using a fluorescein derivative of monoyne **2a**.[14] The comparable reactivity of diyne **3** and monoyne **2a** (R = H) was also supported by the competition experiment,[26] as well as kinetic[27] and computational studies.[28]

In conclusion, we have demonstrated the practical utility of the Sondheimer diyne **3** as a bisreactive molecular hinge in modification of azido-biomolecules with a functional small azido-compound. Considering the ready availabilities of diyne **3** and diverse functional azido-compounds, the SPDC reaction provides a facile method to prepare various functional biomolecules.

Acknowledgements

The authors thank Ms. Mamie Suzuki (Bio-Technical Center, Technical Department, Tokyo Institute of Technology) for performing MALDI-TOF-MS analyses, and Ms. Masayo Ishikawa (Center for Advanced Materials Analysis (Suzukakedai), Technical Department, Tokyo Institute of Technology) and Ms. Ayako Hosoya for HRMS analyses. This study was partially supported by grant-in-aid from Suntory Institute for Bioorganic Research and The Naito Foundation (TH).

Notes and references

1 H. C. Kolb, M. G. Finn and K. B. Sharpless, *Angew. Chem., Int. Ed.*, 2001, **40**, 2004–2021.
2 (*a*) C. W. Tornøe, C. Christensen and M. Meldal, *J. Org. Chem.*, 2002, **67**, 3057–3064; (*b*) V. V. Rostovtsev, L. G. Green, V. V. Fokin and K. B. Sharpless, *Angew. Chem., Int. Ed.*, 2002, **41**, 2596–2599.
3 For reviews, see: (*a*) *Click Chemistry for Biotechnology and Materials Science*, ed. J. Lahann, John Wiley & Sons, West Sussex, 2009; (*b*) M. Meldal and C. W. Tornøe, *Chem. Rev.*, 2008, **108**, 2952–3015, and references cited therein.
4 E. M. Sletten and C. R. Bertozzi, *Angew. Chem., Int. Ed.*, 2009, **48**, 6974–6998.
5 (*a*) N. J. Agard, J. A. Prescher and C. R. Bertozzi, *J. Am. Chem. Soc.*, 2004, **126**, 15046–15047; (*b*) N. J. Agard, J. M. Baskin, J. A. Prescher, A. Lo and C. R. Bertozzi, *ACS Chem. Biol.*, 2006, **1**, 644–648.
6 G. Wittig and A. Krebs, *Chem. Ber.*, 1961, **94**, 3260–3275.
7 (*a*) J. M. Baskin, J. A. Prescher, S. T. Laughlin, N. J. Agard, P. V. Chang, I. A. Miller, A. Lo, J. A. Codelli and C. R. Bertozzi, *Proc. Natl. Acad. Sci. U. S. A.*, 2007, **104**, 16793–16797; (*b*) J. A. Codelli,

J. M. Baskin, N. J. Agard and C. R. Bertozzi, *J. Am. Chem. Soc.*, 2008, **130**, 11486–11493; (*c*) S. T. Laughlin, J. M. Baskin, S. L. Amacher and C. R. Bertozzi, *Science*, 2008, **320**, 664–667; (*d*) S. T. Laughlin and C. R. Bertozzi, *ACS Chem. Biol.*, 2009, **4**, 1068–1072; (*e*) P. V. Chang, J. A. Prescher, E. M. Sletten, J. M. Baskin, I. A. Miller, N. J. Agard, A. Lo and C. R. Bertozzi, *Proc. Natl. Acad. Sci. U. S. A.*, 2010, **107**, 1821–1826; (*f*) J. C. Jewett, E. M. Sletten and C. R. Bertozzi, *J. Am. Chem. Soc.*, 2010, **132**, 3688–3690; (*g*) J. M. Baskin, K. W. Dehnert, S. T. Laughlin, S. L. Amacher and C. R. Bertozzi, *Proc. Natl. Acad. Sci. U. S. A.*, 2010, **107**, 10360–10365; For reviews, see: (*h*) C. R. Becer, R. Hoogenboom and U. S. Schubert, *Angew. Chem., Int. Ed.*, 2009, **48**, 4900–4908; (*i*) M. F. Debets, C. W. J. van der Doelen, F. P. J. T. Rutjes and F. L. van Delft, *ChemBioChem*, 2010, **11**, 1168–1184; (*j*) J. C. Jewett and C. R. Bertozzi, *Chem. Soc. Rev.*, 2010, **39**, 1272–1279.

8 (*a*) X. Ning, J. Guo, M. A. Wolfert and G.-J. Boons, *Angew. Chem., Int. Ed.*, 2008, **47**, 2253–2255; (*b*) A. A. Poloukhtine, N. E. Mbua, M. A. Wolfert, G.-J. Boons and V. V. Popik, *J. Am. Chem. Soc.*, 2009, **131**, 15769–15776.

9 M. F. Debets, S. S. van Berkel, S. Schoffelen, F. P. J. T. Rutjes, J. C. M. van Hest and F. L. van Delft, *Chem. Commun.*, 2010, **46**, 97–99.

10 H. N. C. Wong, P. J. Garratt and F. Sondheimer, *J. Am. Chem. Soc.*, 1974, **96**, 5604–5605.

11 (*a*) A. Orita, D. Hasegawa, T. Nakano and J. Otera, *Chem.–Eur. J.*, 2002, **8**, 2000–2004; (*b*) S. Chaffins, M. Brettreich and F. Wudl, *Synthesis*, 2002, 1191–1194.

12 R. Destro, T. Pilati and M. Simonetta, *J. Am. Chem. Soc.*, 1975, **97**, 658–659.

13 (*a*) H. N. C. Wong and F. Sondheimer, *Tetrahedron*, 1981, **37**, 99–109; (*b*) H. Durr, G. Klauck, K. Peters and H. G. von Schnering, *Angew. Chem., Int. Ed. Engl.*, 1983, **22**, 332–333; (*c*) Y.-M. Man, T. C. W. Mak and H. N. C. Wong, *J. Org. Chem.*, 1990, **55**, 3214–3221.

14 See the Supplementary Information (ESI) for the details.

15 The X-ray crystallographic data for compounds **6a** (CCDC 759900), **6b** (CCDC 759901), **6c** (CCDC 759898), **6d** (CCDC 759899), **7a** (CCDC 759902), **7b** (759903), **7c** (CCDC 759905) and **7d** (CCDC 759904) can be obtained free of charge from the Cambridge Crystallographic Data Centre (CCDC) *via* www.ccdc.cam.ac.uk/data_request/cif. See ESI.

16 The geometries of **6e** and **7e** were confirmed by their reduction ($LiAlH_4$/THF) to the corresponding diols **6d** and **7d**, respectively.

17 K. Chenoweth, D. Chenoweth and W. A. Goddard III, *Org. Biomol. Chem.*, 2009, **7**, 5255–5258.

18 Calculations based on distortion/interaction model showed the similar trend. See ESI. For, distortion/interaction model, see F. Schoenebeck, D. H. Ess, G. O. Jones and K. N. Houk, *J. Am. Chem. Soc.*, 2009, **131**, 8121–8133, and references cited therein.

19 (*a*) J. T. Ngo, J. A. Champion, A. Mahdavi, I. C. Tanrikulu, K. E. Beatty, R. E. Connor, T. H. Yoo, D. C. Dieterich, E. M. Schuman and D. A. Tirrell, *Nat. Chem. Biol.*, 2009, **5**, 715–717; (*b*) A. J. de Graaf, M. Kooijman, W. E. Hennink and E. Mastrobattista, *Bioconjugate Chem.*, 2009, **20**, 1281–1295, and references cited therein.

20 (*a*) T. Hosoya, T. Hiramatsu, T. Ikemoto, M. Nakanishi, H. Aoyama, A. Hosoya, T. Iwata, K. Maruyama, M. Endo and M. Suzuki, *Org. Biomol. Chem.*, 2004, **2**, 637–641; (*b*) T. Hosoya, T. Hiramatsu, T. Ikemoto, H. Aoyama, T. Ohmae, M. Endo and M. Suzuki, *Bioorg. Med. Chem. Lett.*, 2005, **15**, 1289–1294; (*c*) T. Ikemoto, T. Hosoya, K. Takata, H. Aoyama, T. Hiramatsu, H. Onoe, M. Suzuki and M. Endo, *Diabetes*, 2009, **58**, 2802–2812; (*d*) R. Kohta, Y. Kotake, T. Hosoya, T. Hiramatsu, Y. Otsubo, H. Koyama, Y. Hirokane, Y. Yokoyama, H. Ikeshoji, K. Oofusa, M. Suzuki and S. Ohta, *J. Neurochem.*, 2010, DOI: 10.1111/j.1471-4159.2010.06576.x.

21 (*a*) Y. Zhang, M.-k. So, A. M. Loening, H. Yao, S. S. Gambhir and J. Rao, *Angew. Chem., Int. Ed.*, 2006, **45**, 4936–4940; (*b*) G. V. Los, L. P. Encell, M. G. McDougall, D. D. Hartzell, N. Karassina, C. Zimprich, M. G. Wood, R. Learish, R. F. Ohana, M. Urh, D. Simpson, J. Mendez, K. Zimmerman, P. Otto, G. Vidugiris, J. Zhu, A. Darzins, D. H. Klaubert, R. F. Bulleit and K. V. Wood, *ACS Chem. Biol.*, 2008, **3**, 373–382.

22 The increase of molecular weight of the protein at each step was clearly confirmed by MALDI-TOF-MS analysis. See ESI.

23 The labeling efficiency was estimated by comparing the fluorescence intensity with that of HaloTag protein labeled directly with TESRA-HaloTag ligand (**10**) (Fig. 3(b), lane 2), in which the labeling mostly proceeded as judged by MALDI-TOF-MS analysis. See ESI.

24 (*a*) E. Saxon and C. R. Bertozzi, *Science*, 2000, **287**, 2007–2010; (*b*) S. T. Laughlin and C. R. Bertozzi, *Nat. Protoc.*, 2007, **2**, 2930–2944; (*c*) S. T. Laughlin and C. R. Bertozzi, *Proc. Natl. Acad. Sci. U. S. A.*, 2009, **106**, 12–17.

25 A dose-dependent increase in fluorescence intensity by **9** (0 to 40 μM) was observed. See ESI.

26 Stirring equimolar amounts of diyne **3**, monoyne **2a** (R = H) and benzyl azide (**4a**) in methanol (24 h, r.t.) gave bis-cycloadducts **6a**/**7a** and mono-cycloadducts, coupled products of **2a** and **4a**, in approximately 1 : 1 molar ratio. See ESI.

27 The first cycloaddition is the rate-determining step of the SPDC reaction. The second-order rate constant for the reaction of diyne **3** with benzyl azide (**4a**) was determined to be (6.29 ± 0.05) × 10^{-2} M^{-1} s^{-1} (MeOH, 25 °C) by monitoring the time-dependent decrease of absorbance of **3** in the presence of excess amounts of **4a**. It was comparable to that of reported monoyne **2a** (R = H), (5.67 ± 0.27) × 10^{-2} M^{-1} s^{-1} (MeOH, 25 °C). See ESI and ref. 8b.

28 The activation energies for cycloaddition of monoyne **2a** (R = H) with methyl azide (**4f**) were within +11.9 to +14.0 kcal mol^{-1}, which were comparable to that for the first cycloaddition of diyne **3** with **4f**. See ESI and ref. 17.

OPEN ACCESS Freely available online

PLoS one

Splicing Reporter Mice Revealed the Evolutionally Conserved Switching Mechanism of Tissue-Specific Alternative Exon Selection

Akihide Takeuchi[1,3], Motoyasu Hosokawa[2], Takayuki Nojima[1,2], Masatoshi Hagiwara[1,2,3]*

1 Department of Functional Genomics, Medical Research Institute, Tokyo Medical and Dental University, Bunkyo-ku, Tokyo, Japan, **2** Laboratory of Gene Expression, School of Biomedical Science, Tokyo Medical and Dental University, Bunkyo-ku, Tokyo, Japan, **3** Department of Anatomy and Developmental Biology, Kyoto University Graduate School of Medicine, Sakyo-ku, Kyoto, Japan

Abstract

Since alternative splicing of pre-mRNAs is essential for generating tissue-specific diversity in proteome, elucidating its regulatory mechanism is indispensable to understand developmental process or tissue-specific functions. We have been focusing on tissue-specific regulation of mutually exclusive selection of alternative exons because this implies the typical molecular mechanism of alternative splicing regulation and also can be good examples to elicit general rule of "splice code". So far, mutually exclusive splicing regulation has been explained by the outcome from the balance of multiple regulators that enhance or repress either of alternative exons discretely. However, this "balance" model is open to questions of how to ensure the selection of only one appropriate exon out of several candidates and how to switch them. To answer these questions, we generated an original bichromatic fluorescent splicing reporter system for mammals using fibroblast growth factor-receptor 2 (FGFR2) gene as model. By using this splicing reporter, we demonstrated that FGFR2 gene is regulated by the "switch-like" mechanism, in which key regulators modify the ordered splice-site recognition of two mutually exclusive exons, eventually ensure single exon selection and their distinct switching. Also this finding elucidated the evolutionally conserved "splice code," in which combination of tissue-specific and broadly expressed RNA binding proteins regulate alternative splicing of specific gene in a tissue-specific manner. These findings provide the significant cue to understand how a number of spliced genes are regulated in various tissue-specific manners by a limited number of regulators, eventually to understand developmental process or tissue-specific functions.

Citation: Takeuchi A, Hosokawa M, Nojima T, Hagiwara M (2010) Splicing Reporter Mice Revealed the Evolutionally Conserved Switching Mechanism of Tissue-Specific Alternative Exon Selection. PLoS ONE 5(6): e10946. doi:10.1371/journal.pone.0010946

Editor: Stefan Maas, Lehigh University, United States of America

Received February 2, 2010; **Accepted** May 10, 2010; **Published** June 3, 2010

Funding: This work was supported by Grants-in-Aid for Science Research from the Ministry of Education, Culture, Sports, Science and Technology (MEXT) of Japan (to A.T. and M.H.), Japan Science and Technology Agency (JST) (to M.H), New Energy and Industrial Technology Development Organization (NEDO) (to M.H), and the National Institute of Biomedical Innovation (NIBI) (to M.H). The funders had no role in study design, data collection and analysis, decision to publish, or preparation of the manuscript.

Competing Interests: The authors have declared that no competing interests exist.

* E-mail: m.hagiwara.end@mri.tmd.ac.jp

Introduction

Genome projects have shown that metazoans generate a hugely diverse proteome from a limited number of genes. This finding underscores the importance of alternative splicing, through which a single gene can generate multiple structurally and functionally distinct protein isoforms. Moreover, recent transcriptome analyses with splicing-sensitive microarrays or deep sequencers have revealed that alternative splicing occurs in more than 90% of multi-exon genes in human [1] and over 60% of these cases are regulated in a tissue- and cell type-specific manner [2]. Alternative splicing is regulated by auxiliary cis-elements with regulatory proteins that enhance or repress splicing of adjacent exons [3,4] however, the mechanism by which a number of genes are regulated in various tissue-specific manner by a limited number of regulatory factors remains unclear.

In mammals, fibroblast growth factor-receptor 2 (FGFR2) is one of the best characterized gene in which mutually exclusive alternative splicing produces two isoforms. Exon 8 (also termed IIIb) isoform is specifically expressed in epithelial tissues, whereas exon 9 (or IIIc) isoform is selected in non-epithelial or mesenchymal tissues [5,6]. The structural difference between two splice isoforms markedly affects the specificity of ligand–receptor binding [7,8,9], and exon switching is shown to be essential for development in the mouse [10,11]. Several factors have been identified which positively or negatively regulate either of alternative exons of FGFR2 independently. For exon 8 regulation, Del Gatto-Konczak et al. found that heterogeneous nuclear ribonucleoprotein, hnRNP A1, binds to exon 8 (also termed K-SAM exon) as ESS (exonic splicing silencer) and represses its inclusion [12]. Carstens et al. found the polypyrimidine tract binding protein (PTB) represses exon 8 inclusion through ISS-1 and ISS-2 (intronic splicing silencers-1 and 2) [13]. Warzecha et al. recently cloned RBM35a and RBM35b as epithelia-specific activators of exon 8 inclusion, and renamed them epithelial splicing regulatory proteins 1 and 2 (ESRP1 and ESPR2), respectively [14]. For exon 9 regualtion, Chen et al. found that Tra2β represses the selection of exon 9 [15]. Baraniak et al. reported that Fox2 represses selection of exon 9 through binding to a UGCAUG sequence in intron 8 [16]. Hovhannisyan

et al. found that a hnRNP M binds to ISS-3 and represses inclusion of exon 9 [17]. Mauger et al. showed that hnRNP H and F interact with Fox2 and repress exon 9 inclusion [18]. Also, presence of unknown enhancer is speculated for exon 9 inclusion through ISE (intronic splicing enhancer) in intron 9 [14]. So far, mutually exclusive splicing regulation is widely believed as the outcome from the balance of multiple regulators that enhance or repress either of alternative exons discretely [19,20]. However, this "balance" model is open to questions, 1) How the balance of multiple regulators can ensures the selection of only one appropriate exon out of several candidates? 2) Whether transcriptional or post-transcriptional control of multiple regulators is possible to achieve distinct switching of alternative exons? 3) If 2) is the case, how to control the multiple regulators at once for exon switching? To answer these questions, we generated a bichromatic fluorescent splicing reporter system for mammals using FGFR2 gene as a model. This reporter contains entire cis-elements necessary to reproduce native alternative splicing regulation and enable us to visualize and monitor it *in vitro* and *in vivo*. The transgenic mice expressing this splicing reporter clearly showed the epithelial tissue-specific splicing pattern throughout their entire bodies. By using this splicing reporter, we demonstrate that key regulators define the single exon expression in the tissue-dependent manner through the ordered splice-site recognition of the mutually exclusive exons.

Results

Generation of the FGFR2 splicing reporter system

We used a 3.7-kb genomic fragment of FGFR2 gene that included two alternative exons (exon 8 and 9) flanked by their upstream and downstream exons (exon 7 and 10), with introns in between (Figure 1A). By using mostly entire genomic region around alternative exons, this reporter system was expected to contain all the regulatory cis-elements essential for tissue-specific regulation and to tell which splice site sequences and cis-elements are truly critical for regulations. The genomic fragment was cloned into a vector containing RFP and EGFP in tandem with different reading frames [21]. With this reporter system, splicing regulation could be monitored from a single reporter vector that expresses either EGFP when exon 8 is chosen or RFP when exon 9 is selected (Figure 1A).

By using two prostate carcinoma cell lines, AT-3 and DT-3 cells, we then examined whether the reporter system could reflect cell type-specific splicing regulation. AT-3 cell is a mesenchymal-type cell that specifically expresses exon 9 isoform of endogenous FGFR2, and DT-3 cell is an epithelial-type cell that predominantly expresses exon 8 isoform [22]. When this reporter system was introduced into these two cell lines, AT-3 cell specifically expressed exon 9-RFP and DT-3 cell predominantly expressed exon 8-EGFP (Figure 1B). We therefore could confirm that our reporter vector reflects cell type-specific regulation of endogenous FGFR2 splicing.

We next checked whether our reporter system could show tissue-specific regulation of FGFR2 splicing in vivo by generating transgenic mice from this reporter. A well-known change in the FGFR2 splicing isoforms occurs in mouse development stages from E14.5 to E16.5. In these stages, differentiation of future epithelial cells is induced and they start expressing exon 8 isoform of FGFR2 to receive morphogen signals, such as FGF-10, from mesenchymal cells [23]. When the whole body of a transgenic embryo was examined at E14.5, a broad RFP signal was detected throughout the entire body, and a specific EGFP signal was detected as the whisker pattern and on the edges of limbs or the body (Figure 1C). We further evaluated the detailed expression profile through examining series of sections from the transgenic embryos in the late development stage of E16.5 (Figure 1D). An EGFP signal was detected specifically in cells on the surface of the skin and bulbs of hair follicles, where differentiated epithelial cells were located (Figure 1D, shown with arrows). Also, the EGFP signal was detected at epithelial cells in the alveoli of the lung, in the esophagus and colon, at the thymus epithelia, and at the salivary gland ductal cells (Figure 1D, arrows in the top and middle panels). A strong RFP signal was detected in the developing brain (hippocampus) and peripheral nervous system (trigeminal ganglia) (Figure 1D, arrows in bottom panels). Expression patterns of EGFP were compatible with reported FGFR2 exon 8 expression patterns [23,24], indicating that our reporter system reflects endogenous splicing regulation of FGFR2 in vivo and the genomic fragment used in the vector contains the regulatory elements necessary for tissue-specific switching of mutually exclusive exons.

Unbalanced sequence of 3′ splice site is essential for mutually exclusive exon selection

In the embryos of splicing reporter transgenic mouse, RFP was expressed almost throughout the entire body, and EGFP was specifically expressed in epithelial cells. This expression pattern suggested the possible regulatory mechanism that exon 9 was dominantly selected as "default" in reporter transgenic mouse, and epithelial-specific regulators might promote inclusion of exon 8. To test this hypothesis, we initially compared sequence of alternative exons including their 3′ and 5′ splice sites. The major difference identified between these two exons is that exon 8 has a weaker 3′ splice site and a polypyrimidine moiety that contains several mismatches from the consensus sequence (Figure 2A, TGTTCTAG ca), whereas exon 9 has stronger 3′ splice site which has conserved consensus sequences (Figure 2A, TTTTCTAG gc). There are no obvious differences in their 5′ splice sites (data not shown). To examine whether the unbalanced 3′ splice site is essential for "default" selection of exon 9 in non-epithelial cells, we introduced mutations in their 3′ splice sites and observed change in splicing regulations. We prepared two types of mutated vectors, one has the same stronger 3′ splice sites on both exon 8 and 9 (Figure 2A, E8-S vector), and the other has the same weaker 3′ splice sites on both exon 8 and 9 (Figure 2A, E9-W vector). These vectors were transfected into AT-3 and DT-3 cells, and the change of splicing regulation was examined by RT-PCR. When WT vector was introduced into AT-3 cell, it adopted almost 100% of the exon 9 form, whereas DT-3 cell adopted around 45% {34.5/(34.5+42.7)%} of exon 8 form among the single inclusion product (Figure 2B, lane 1, 4), which was consistent with the expression pattern of fluorescence in Figure 1B. Our splicing reporter was designed not to cause early premature termination codon in double-inclusion form to escape the nonsense-mediated decay (NMD) reaction [25]. We therefore could monitor all splicing products, including the double-inclusion and the double-skip forms. Strikingly, when E8-S vectors were transfected, AT-3 cell mostly expressed the double-inclusion form, meaning that two alternative exons were processed as constitutive exons (Figure 2B, lane 2). This result indicates that the weaker 3′ splice site of exon 8 is critical for single exon selection of exon 9 from two mutually exclusive exons in non-epithelial AT-3 cell (Figure 2B, lane 2), though the ESS or ISS on or close to exon 8 may be required for the complete suppression [13,26,27]. When the 3′ splice site of exon 9 was weakened (E9-W vector), selection in DT-3 cell almost fully switched to exon 8 (Figure 2B, lane 4 and 6), indicating that full repression of exon 9 might be important for exon 8 inclusion in epithelial DT-3 cell. Thus unbalanced 3′ splice sites are essential for the single exon choice from mutually exclusive exons and for their switching.

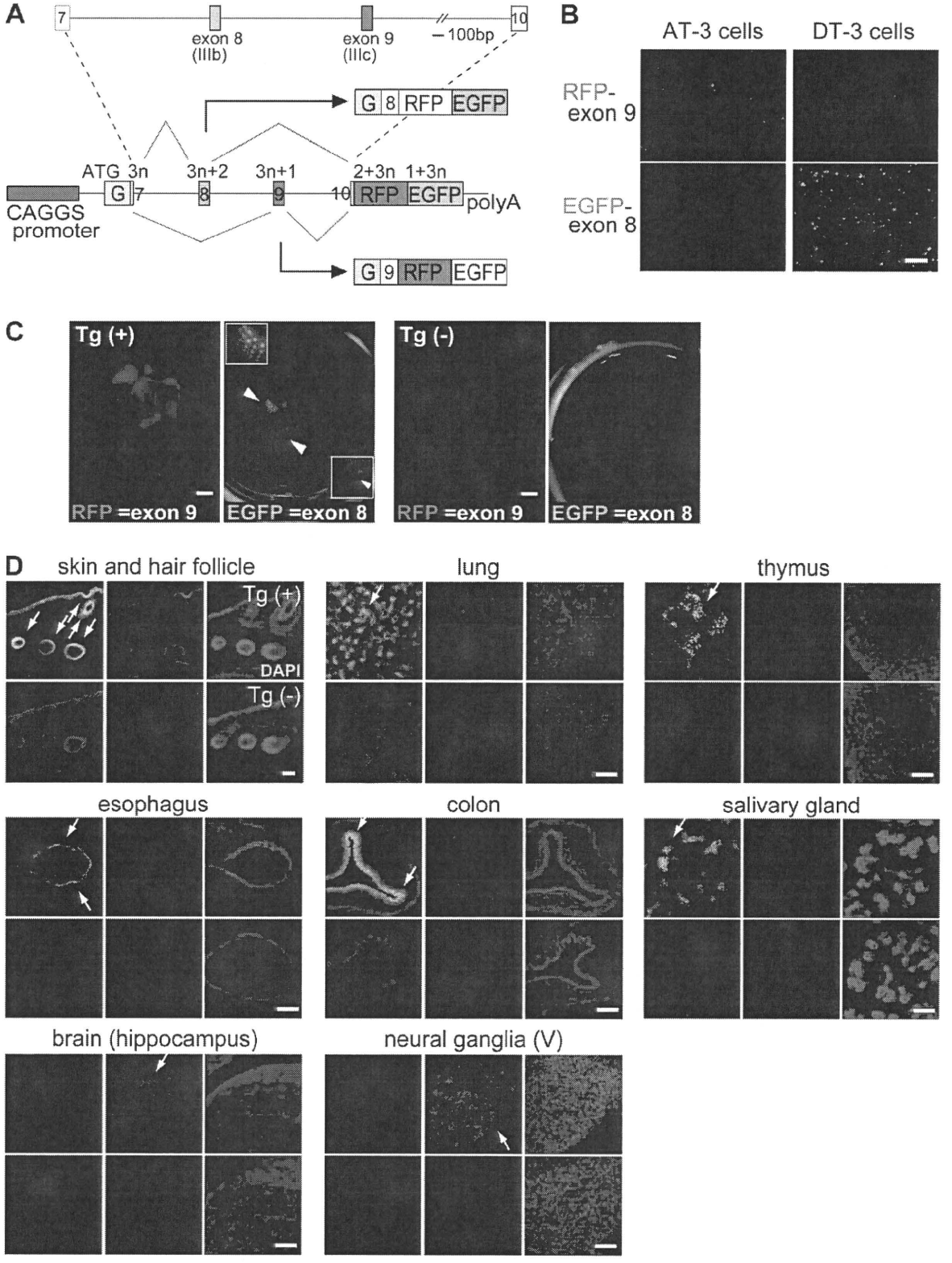
A
7
exon 8
(IIIb)
exon 9
(IIIc)
100bp
10
G 8 RFP EGFP
ATG 3n
3n+2
3n+1
2+3n 1+3n
G 7 8 9 10 RFP EGFP
polyA
CAGGS
promoter
G 9 RFP EGFP
B
AT-3 cells
DT-3 cells
RFP-
exon 9
EGFP-
exon 8
C
Tg (+)
RFP =exon 9
EGFP =exon 8
Tg (-)
RFP =exon 9
EGFP =exon 8
D
skin and hair follicle
Tg (+)
DAPI
Tg (-)
lung
thymus
esophagus
colon
salivary gland
brain (hippocampus)
neural ganglia (V)

Figure 1. Construction of FGFR2 splicing reporter vector and their expression patterns. (A) Scheme of FGFR2 splicing reporter vector. The genomic fragment of mouse FGFR2 including exon 7 through 10 was amplified and introduced into the reporter vector containing a CAGGS promoter and RFP-EGFP with different reading frames. Modified glutathione-S-transferase gene (indicated as "G") was inserted in front of the exon 7 in-frame. A schematic representation of the mRNA derived from the reporter under the alternative splicing regulation is also shown; the numbers indicate the reading frames. (B) Expression pattern of splicing reporter in vitro. The reporter vector was introduced into two rat prostate cancer cell lines AT-3 and DT-3, which have different cell-type specificities. Scale = 200 μm. (C) Expression pattern of splicing reporter in vivo. Fluorescence images of transgenic reporter mouse embryos at E14.5. Tg(+) is an embryo carrying the reporter vector, and Tg(−) is one of its litter-mate lacking the vector. Arrowheads in Tg(+) indicate EGFP signals with the patterns of whiskers (upper arrowhead) and the edge of a limb (lower arrowhead), both of which are magnified and indicated by white rectangles in the upper left-hand and lower right-hand corners, respectively (scale = 1 mm). (D) Sections from transgenic reporter mouse embryos at E16.5. Each panel shows sections from the indicated tissues, the upper one from Tg(+) and the lower from Tg(−). Portions expressing the EGFP signal are indicated by white arrows (scale = 100 μm).
doi:10.1371/journal.pone.0010946.g001

Disruption of exon 9 causes switching to exon 8

Results in Figure 2 showed that weaker 3' splice sites of exon 8 is essential for the single exon selection of exon 9 in non-epithelial AT-3 cell. And epithelial DT-3 cell efficiently chose exon 8 form when 3′ splice site of exon 9 was weakened. These observations suggest a possibility that repression of exon 9 causes switching to exon 8. To examine this hypothesis, we introduced mutations on either or both of the 3' and 5' splice sites of exon 9 to destroy its splice site consensus sequence mimicking repression, and transfected these into AT-3 cell (Figure 3A). When both splice sites of exon 9 were mutated (Figure 3A, 3′&5′ ss Mut), AT-3 cell expressed the exon 8 form (22.9%) and the double-skip form (77.1%) (Figure 3B, lane 4). These results indicated that blocking of exon 9, at least partially, promotes switching to exon 8 in AT-3 cell. Interestingly, mutation of the 3' splice site (Figure 3A, 3′ ss Mut) was just sufficient to cause this switching (Figure 3B, lane 2), whereas mutation of the 5' splice site (Figure 3A, 5′ ss Mut) produced an aberrant splicing product of exon 9 using a cryptic 5' splice site at ggGT in exon 9 (Figure 3B, lane 3 indicated by arrowhead and scheme was illustrated on the right side). These results indicate that recognition of 3′ splice site is essential for exon 9 selection, suggesting the possibility that recognition of exon 9 is its 3′ splice site dependent. To test this hypothesis, we performed in vitro splicing assay to directly monitor the splice site recognition by U2 and U1 snRNA/snRNP binding (Figure 3C). The ^{32}P-labeled RNA probes for wild-type and mutated exon 9 containing the flanking introns (top panels of Figure 3C) were crosslinked by UV irradiation after incubation with HeLa nuclear extract and separated by electrophoresis. HeLa cell was confirmed to have non-epithelial cell character. The specificity of U2 or U1 binding was confirmed by addition of an oligonucleotide complementary to U2 or U1, and RNase H digestion [28,29] (Figure 3C and Figure S1). In the splicing conditions, binding and shift of U1 and U2 snRNAs were observed with the WT RNA probe, in which the U1 and U2 bands overlap (Figure 3C, lane 1–4, and Figure S1, lane 1–4, indicated by an arrow). They became fainter by RNase H digestion with U1 (Figure 3C, lane 3, and Figure S1, lane 3) or U2 oligos (Figure 3C, lane 4, and Figure S1, lane 4). Shifted band almost disappeared with double digestion with U1+U2 oligos (Figure S1, lane 7), while the band was resistant against the RNase H digestion with U6 oligo (Figure S1, lane 8), indicating that the exon 9 RNA probe is recognized by U1 and U2 oligos in this splicing condition. Strikingly, the 3' splice site mutation of the exon 9 RNA probe resulted in a significant loss of the shifted band (Figure 3C, lane 6–8). These results suggested that recognition of exon 9 primary depends on the binding of U2 snRNA to the 3' splice site. On the contrary, with the probe harboring with 5' splice site mutation (5' ss mutation), binding of both U1 and U2 was retained (Figure 3C, lane 10–12), in good accordance with the results of RT-PCR shown in Figure 3B, lane 3. These results suggest a possibility that binding of U2 snRNA supports the binding of U1 snRNA, so that much weaker cryptic 5' splice sites in exon 9 was used in its 5′ ss mutation (Figure 3B, lane 3 and Figure 3C, lane 12 indicated by an arrowhead with an asterisk). These observations give a possible explanation why the selective use of exon 9 in non-epithelial cells depends on the relative strength of its 3' splice site.

Identification of silencing elements for exon 9 recognition

Non-Epithelial or Mesenchymal regulation, unbalanced 3' splice sites are essential for single exon selection of exon 9 in non-epithelial cells and recognition of exon 9 is its 3′ splice site dependent. Also disruption of this 3' splice site of exon 9 partially caused switching to exon 8. These results suggest the presence of silencer(s) for exon 9 to cause switching to exon 8 in epithelial cell. To test this hypothesis, we initially screened suppressive cis-elements located near the 3' splice site of exon 9, and picked up two highly conserved sequences: the UGCAUG sequence and ISE/ISS-3 (intronic splicing enhancer/silencer-3) in intron 8, both of which have been reported as the silencing cis-elements for exon 9 [16,30] (Figure 4A). To examine whether these two cis-elements are essential for silencing exon 9, we introduced mutations in either or both UGCAUG and ISE/ISS-3 in our reporter, and transfected into epithelial DT-3 cell. First, we substituted UGCAUGCAUG for UACGUACGUG to disrupt the binding to the RNA-binding protein of Fox, which was reported as the repressor of exon 9 [16]. Then, the ratio of exon 8 selection in DT-3 cell fell by a half (44.7% to 21.9%, Figure 4B, lane 2). Next, we deleted ISE/ISS-3, an 85-bp sequence containing several dinucleotide GU sequences. The deletion of ISE/ISS-3 reduced the ratio of exon 8 inclusion to one-fourth (44.7% to 12.4%, Figure 4B, lane 3). When both of these elements were mutated, DT-3 cell could no longer choose exon 8, and all splicing products were the exon 9 form (Figure 4B, lane 4). These results indicate that DT-3 cell use both of these cis-elements to select exon 8 presumably by silencing the exon 9 via its 3' splice site.

Regulatory mechanism of transacting factors to switch exons

Results from Figure 4 suggest that both UGCAUG and ISE/ISS-3 are necessary and sufficient for selecting exon 8. A previous study has shown that Fox2 promotes exon 8 inclusion through UGCAUG in intron 8 [16]. Also, a recent study from cDNA library screening identified epithelial splicing regulatory protein ESRP1 and ESRP2, which mediate exon 8 inclusion through binding to ISE/ISS-3 [14]. We therefore examined whether Fox1, Fox2, ESRP1, and ESRP2 promote switching from exon 9 to exon 8. First, we examined and compared the expression levels of these RNA-binding proteins between AT-3 and DT-3 cells by RT-PCR. Fox2 was expressed in both cell lines at similar levels, whereas expression of Fox1 was undetectable (Figure 4C), and both ESRP1 and ESRP2 were specifically expressed in epithelial type DT-3 cell (Figure 4C). Considering the observation that both UGCAUG and

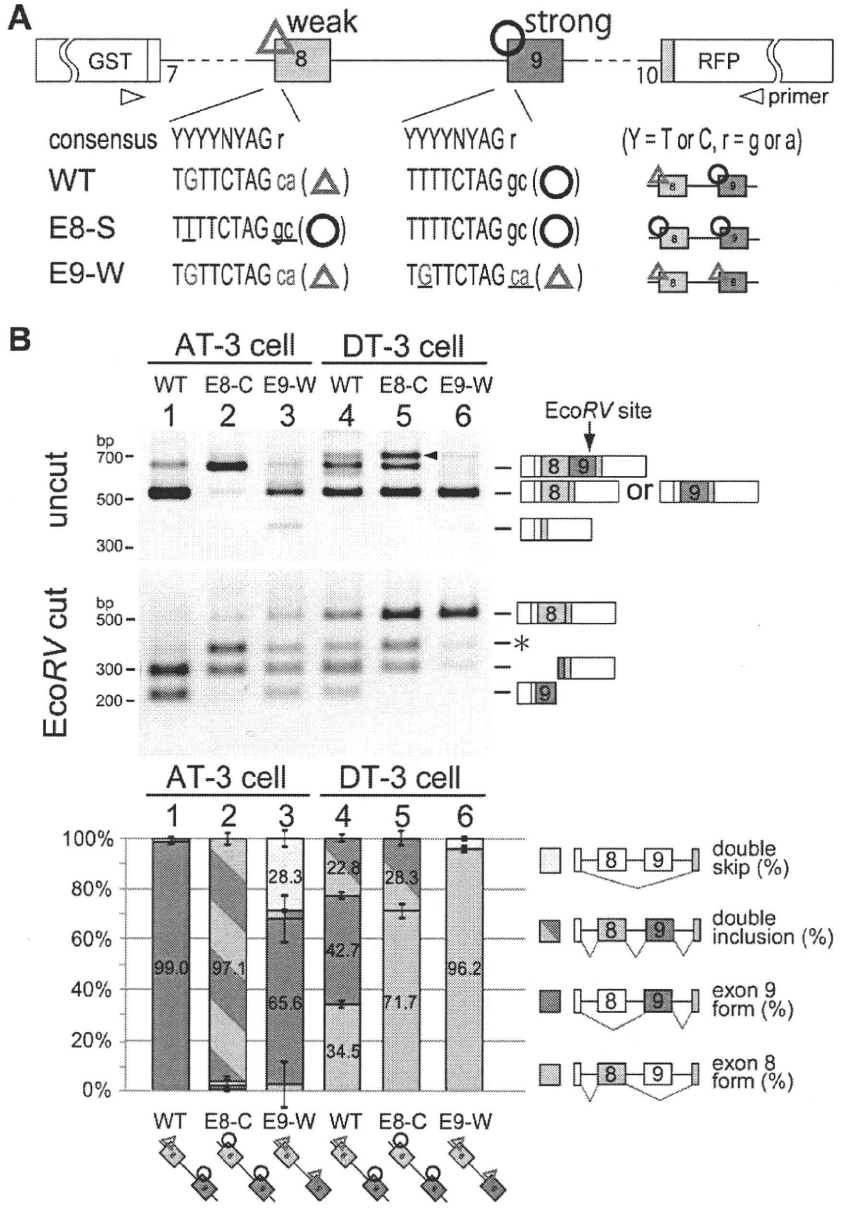

Figure 2. Unbalanced sequence of 3′ splice sites is essential for mutually exclusive exon selection. (A) Scheme for 3′ splice site mutation on exons 8 and 9. Uppercase letter is intron and lowercase is exon sequence. Red characters indicate mismatches from the conserved consensus sequence in the 3′ splice site and poly-pyrimidine moiety, and underline indicate mutated sequence. The yellow arrows with "primer" represent the positions amplified in RT-PCR. (B) RT-PCR from AT-3 and DT-3 cells transfected the indicated vectors. Splice products were digested with Eco*RV*, which uniquely cuts the PCR product containing exon 9. Each band was identified and indicated with the scheme of splice products. Arrowheads indicate nonspecific PCR products, which was confirmed by sequencing. The asterisk indicates the splice product came from double inclusion of exon 8 and exon 9. The bar graph shows the amount of each splicing product, and is based on calculations from three independent experiments; the mean value for each splice product is show in the respective column with an error bar showing the SD (standard error).
doi:10.1371/journal.pone.0010946.g002

ISE/ISS-3 are essential cie-elements for selecting exon 8 (Figure 4B), broadly expressed Fox2 might cooperates with epithelial-specific ESRP1 and ESRP2 for exon 8 inclusion. To test this hypothesis, we transfected our FGFR2 splicing reporter with Fox1, Fox2, ESRP1, or ESRP2, or combinations of these into HeLa cell, which has non-epithelial cell character (Figure 5A, lane 1).

When Fox1 or Fox2 was introduced into HeLa cell, selection of exon 8 increased in a dose-depend manner and reached 10% (Figure 5A, lanes 2–4) or 40% (Figure 5A, lanes 5–7), respectively.